FABRICATION OF A MICROCHIP DEVICE FOR LIQUID PHASE ION MOBILITY SPECTROMETRY

By

NAZMUL HUDA AL MAMUN

A thesis submitted in partial fulfillment of
the requirements for the degree of

MASTER OF SCIENCE IN MECHNICAL ENGINEERING

WASHINGTON STATE UNIVERSITY
School of Mechanical and Materials Engineering

DECEMBER 2006

To the Faculty of Washington State University:

The members of the Committee appointed to examine the thesis of NAZMUL HUDA AL MAMUN find it satisfactory and recommend that it be accepted.

_____
Chair

_____

_____

ACKNOWLEDGMENT

The author wishes to express his deep gratitude and indebtedness to Dr. Prashanta Dutta, Assistant Professor of School of Mechanical and Materials Engineering (MME) at Washington State University (WSU), Pullman for this supervision, valuable suggestions, guidance, and constructive criticism throughout this investigation and for patiently reading the manuscript and suggesting its improvement.

The author is greatly indebted to Dr. Herbert H. Hill Jr., Professor of the Department of Chemistry at Washington State University, Pullman and the inventor of this cutting edge liquid phase ion mobility spectrometry research, for his valuable suggestion, guidance, and providing instruments. The author feels extremely proud to work in his guidance.

The author is exceedingly grateful to Dr. Robert F. Richards for giving his kind consent to be on the committee and support on different issues.

Special thanks to Mr. Robert Lentz for taking time out of his busy schedule to provide support during this research work. Thanks to Ms. Mary Simonsen, Ex. Graduate Program Coordinator of School of MME at WSU, for all her help.

The author would like to thank Maggie Tam, Graduate student of the Chemistry Department, for all her support during this work in Dr. Hill's lab. Special thanks to friends and the people the author met at this institution for making the clean room work cheerful and this stage of life memorable.

This work was supported partially by National Science Foundation and National Institutes of Health. Contributions from these two sources are greatly appreciated.

Finally the author would like to thank his parents and sisters for all of their emotional and financial support and for helping the author achieve his goals.

FABRICATION OF A MICROCHIP DEVICE FOR LIQUID PHASE ION MOBILITY SPCETROMETRY

Abstract

by Nazmul Huda Al Mamun, M.S.
Washington State University
December 2006

Chair: Prashanta Dutta

A polymer based microfluidic chip has been developed to generate and detect ions from different chemical samples for liquid phase ion mobility spectrometry. This is a device which integrates both the ionization source and the detection part in the same module for lab-on-a-chip applications. The fluidic part consists of a nozzle (12 μm deep) and a drift channel (400 μm deep), which are embedded into the chip made of poly-di-methyl-siloxane (PDMS). Its (PDMS) transparency, insulating properties, and chemical inertness make it indispensable as the device material of electrospray ionization ion mobility spectrometry. Soft lithography and oxygen plasma were used for channel fabrication and bonding respectively.

The electronic part consists of high voltage power supplies, current detection system, and a series of platinum microelectrodes embedded in the nozzle and drift channel. Platinum microelectrodes, being inert to chemicals and bio-molecules, become essential components in microfluidic devices. The biggest challenge of laying down platinum into a deep channel has been overcome by developing a new fabrication procedure. This approach, included in details in this study, can be used for both low and high aspect ratio channels and avoids hazardous chemicals. The depth of the Pt-electrode was measured as 300-400 nm with a surface roughness of ±50 nm.

The continuity of microelectrodes, ionization and detection performance of the developed microchip were investigated. A non-polar liquid, benzene, and a polar liquid sample, 90: 10 Methanol: Water, were ionized separately in the microchip. The maximum ion current measured by the detector was approximately 0.7 nA due to sample ionization. It was also observed that benzene was not ionized. In both cases the electrodispersion ionization voltage was 1250 V/mm and the drift (electric) field was 50 V/mm. This ensures the continuity of microelectrodes and satisfactorily demonstrates the ionization and detection of ions. Negative and positive ions were detected by the microchip. It was also observed that the increase in drift field increased the ion current probably because the loss of some ions at the channel surface was avoided at a higher drift field.

TABLE OF CONTENTS

Page

LIST OF TABLES

LIST OF FIGURES

Dedication

This dissertation/thesis is dedicated to my mother and father

who provided both emotional and financial support

CHAPTER ONE

INTRODUCTION: MICROFLUIDICS AND ION MOBILITY SPECTROMETRY

1.1 Preliminary

Microfluidics is an interdisciplinary branch of science and technology that deals with the flow of small quantities of liquids or gases- typically measured in micro- and nano- liters- in the miniaturized systems. These systems require new fabrication method adopted from the semiconductor technology to have some physical processes dominant, such as, electro-osmotic movement, surface interactions, etc [Barry and Ivanov, 2004]. A crude idea about microfluidic devices can be given as:

- Typical dimension of the flow path: Comparable with a human hair which is approximately 50μm in diameter;
- Microfluidic chip size: 1 - 50 cm^2;
- Channel dimensions: 1 – 200 μm especially in depth;
- Volume of liquid or gas flows: micro- to nano- liters.

Microfluidic devices have been playing a significant role in recent years in the arena of life sciences. Over the last decade, they have enjoyed a great success in certain applications; among them ink-jet printers are noteworthy. However, recent development and innovations of complex systems of channels with sophisticated fluid flow control have made this technology ubiquitous. Following the trend of miniaturization, this development has brought an enormous impact especially in pharmaceuticals [Reed, 2002], medical analysis [Liu et al., 2006], biotechnology [Barry and Ivanov, 2004], environmental monitoring [Zaytseva et al., 2005], defense [Lim et al., 2005], biochemical analysis [Anderson et al., 1997], agriculture [Scott, 2005], and microchemistry [Boone, 2002].

Several advantages have brought the microfluidic devices into limelight. They require only a small amount of sample and reagent for each process—only a few tens or hundreds of nano liters compared with the 5-10 ml required by existing analytical devices. They reduce the analysis time a lot, only a few seconds, because of faster mixing, separation, and reaction due to small fluid volumes. They enable the analysis systems portable. Microfluidics' appeal also lies in increase in separation resolution, and array density [Ramsey et al., 1995; Sanders et al., 2002]. Microfluidic chips hold the promise of combining multiple functions on a single chip, including purification [Shaikh and Ugaz, 2006], labeling [Helmke and Minerick, 2006], reaction [Verpoorte, 2002], separation [Sanders et al., 2002], and detection [Wang et al., 2003, Salgado et al., 2006]. Integration of multiple analytical steps on a single device requires complex channels with nozzles, pumps, valves, mixers, separators, and detectors (sensors) and leads to the development of so-called "lab-on-a-chip" or "micro-total analytical system (μ-TAS)" [Sanders et al., 2002]. Also automated microfluidic technologies can do routine assays, thus reducing human intervention. Flexibility and cost effectiveness are two important traits that are deemed crucial to the devices' commercial success and give the microfluidic technology a competitive edge in emerging markets.

Among hundreds of exciting applications of microfluidics, miniaturized ion mobility spectrometry (IMS) is one of the recent inventions. The ion mobility spectrometry technique separates and detects electrically charged particles (ions) that have been sorted according to how fast they travel through an electrical field in a tube. Small ions travel very fast, and they reach the detector first, with successively larger ions following along behind. The IMS technology was invented in the late 1960s and early 1970s. Since then its potential as an analytical tool and a sensitive trace detector was realized [Karasek et al., 1971]. However its use as a field monitoring and detection device to ensure a clean and safe environment got more attentions with the production of

miniaturized, handheld, inexpensive IMS instruments. Detection of toxic, hazardous, life threatening chemicals and stack gases are major environmental and industrial applications of IMS instruments. IMS technology is now being used extensively to detect explosives and contraband drugs at airports worldwide. Its high sensitivity, high-speed response, and high confidence level have brought it in the forefront in determinations of chemical warfare agents in the battlefields. Another important factor that has been playing a vital role to popularize the IMS technique is it operates at atmospheric pressure.

1.2 Gas Phase Ion Mobility Spectrometry: Principle of Operation

The operating principle of the ion mobility spectrometry has been demonstrated in Fig. 1.1. Samples, either solid or liquid, are vaporized in an analyzer by thermal desorption. Resulting vapors are then ionized by radioactive or non-radioactive sources in the ionization region to produce ions or molecular ion clusters.

Ions are gated by an electronic shutter into a drift tube. They collide with neutral drift gas molecules at atmospheric pressure while traveling down the drift region due to an electric field along the drift channel. The purpose of the drift gas is to sweep off unwanted species out of the system. Ions then strike the detector and generate an electric current. They are separated according to their size and shape and identified based on detection of peaks at a specified drift time. It is obvious that smaller ions move faster than larger ions due to their smaller cross-sectional areas and hence require less drift time than that of larger ions. This has been shown in Fig. 1.1.

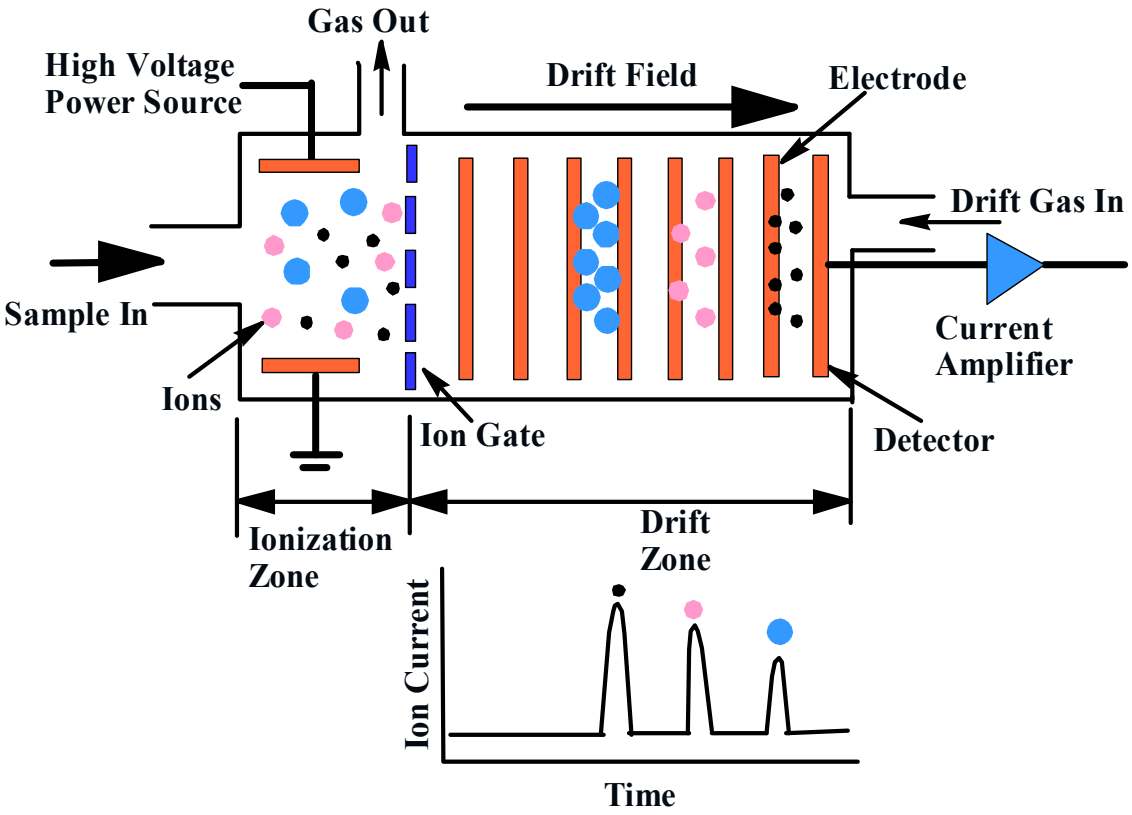

Fig. 1.1 Schematic of the principle of operation of ion mobility spectrometry. Sample vapor is ionized by an ionization source in the ionization zone. Ions are then gated by an electronic shutter into the drift zone. Ions move down the drift region due to the electric field (also known as drift field) and detected by the detector. Smaller ions move faster than larger ions, hence require less drift time.

1.3 Applications

At the end of 1980's, application of IMS/MS (ion mobility spectrometer-mass spectrometer) was first introduced by Karasek et al. [Karasek et al., 1978]. They used ion scattering spectrometry (ISS) and secondary ion mass spectrometry (SIMS) for air pollution monitoring from surfaces. A piece of Al siding with discolored paint, a section of filter paper containing airborne particulate matter, and a heavily corroded bicycle spoke were chosen as characteristic samples of non-ideal surfaces. Manganese and

Mg_2SiO_4 were identified as atmospheric pollutants. ISS demonstrated a detection limit of 1 ng/mm^2 for Cu with a resolution of 0.18 for ^{65}Cu and ^{63}Cu while the SIMS values were 100 and 1.4 pg/mm^2 respectively. This is the pioneer work towards the contribution in ion mobility spectrometry. Carr et al. [Eiceman and Karpas, 1993] used the IMS/MS technology to analyze organic surface contaminants, headspace vapor in sealed electronic packages, and polymer outgassing. They also showed the quantitative H_2O determination in components using IMS/MS. They combined the sensitivity of the IMS and its ease of operation at ambient pressure with the identification capability of mass spectrometry. A review of major areas where attempts have been made to utilize Atmospheric Pressure IMS technology is discussed below.

1.3.1 Biological

IMS technology made it possible to identify and differentiate trees having no bark around them [Lawrence and Barbour, 1991] by analyzing the emanating vapor composition from different species of wood. Snyder et al. [Snyder et al., 1991] showed that IMS could detect the vapor released during the bacterial enzymatic reaction followed by a controlled chemical reaction. Monitoring of microbiotics in solution, particularly in water, was referred from IMS detection as the amount of the released vapor proportional to the amount of microbiotics material present in the solution. Clowers et al. [Clowers et al., 2005] reported a series of isobaric disaccharid-alditols and select trisaccharides using atmospheric pressure ion mobility spectrometry coupled with time-of-flight mass spectrometry. Electrodispersion ionization was used in this investigation.

1.3.2 Environmental and Industrial

Leasure and Eiceman [Leasure and Eiceman, 1985] monitored the chemicals hydrazine and monomethylhydrazine (MMH) using IMS. The detection limits of these compounds were below 10 ppb, which conformed to the threshold limit value (TLV) of

10 ppb adopted by the American Council of Governmental and Industrial Hygienists (ACGIH) in 1995. Hydrazine is a toxic chemical compound used as a rocket fuel. Breathing hydrazines for short periods may cause coughing and irritation of the throat and lungs, convulsions, tremors, or seizures and for long periods may cause liver and kidney damage, as well as serious effects on reproductive organs [websters online dictionary].

Monitoring of HF levels using the IMS-based instrument (FP/ IMS) developed by ETG and marketed by Sensidyne (Clearwater, FL) is one of the most advanced accomplishments of IMS technology in environmental and industrial sector [Bacon et al., 1990, 1991]. Its extensive application could be in refining, semiconductor, and aluminum fabrication industries. This device samples the ambient air by the use of a Venturi suction system (hence gets rid of the pump), and uses a reagent (methylsalicylate) that shifts the reactant ion peak so that it does not interfere with the HF product ion peaks and thus increases sensitivity and specificity [Spangler and Epstein, 1990] . Its sensitivity towards coexisting gases such as NO, H_2S, and NO_2 was found to be quite low and moderate towards HCl and Cl_2 [Bacon et al., 1990]. Its minimum detectable limit is 0.5 ppm and the sensor life in excess of 10 years as per the claim of the manufacturer.

Electrospray ion mobility spectrometry was used by Asbury et al. [Asbury et al., 1999] to analyze chemical warfare degradation products from common nerve agents and sulfur mustard gas. In their investigation, the detection limits were less than 100 ppb for 7 of the 12 compounds.

IMS technology was also introduced to monitor bromine concentration in air [Karpas et al., 1991] and the highly toxic (TLV of 5 ppb) toluene diisocyanate (TDI) [Roehl and Bacon, 1989; Brokenshire et al., 1990]. Though detection of both isomers

(2,4-TDI and 2,6-TDI) were reported at the low-ppb level, interferences from ppm levels of amines (used as catalysts in TDI production) and also some changes in response due to high levels of halogenated compounds were noted.

1.3.3 Explosive Detections

There are two types of detection devices: (i) explosive detection systems (EDSs), which are designed to detect large quantities of explosives based on physical dimensions and densities consistent with explosive materials; and (ii) explosive trace detectors (ETDs), which are used to detect vapor or particles of explosives [seenex]. Among various kinds of ETDs, ion mobility spectrometers are the most commonly used instruments by the security agents to detect telltale traces of chemicals that evaporate from the surfaces of suspected substances. In this section, some of the modern commercial IMS-based instruments used specifically for the detection of explosives will be described.

Barringer Technologies Inc. (now Smiths Detection) developed trace vapor detection systems, which was named Ionscan, utilizing the ion mobility spectrometry technology. Trace detection is the collection and analysis of minute, invisible amounts of substances that are extremely small, neither visible to the naked eye nor easily washed off. Someone who has handled explosives or narcotics will invariably leave traces of those substances on items they subsequently touch. The Ionscan is designed to detect and identify these traces deposited on items such as electronic devices, baggage, cargo, vehicles, buildings, and on the people themselves.

The detection of explosives works as follows: a special cloth, or “swab”, is wiped over the surface of the items in question. It is then placed into the device, where the particles are heated to vaporize. These vaporized substances are then ionized and

allowed to “drift” through a tube. These ions move at different speeds through the tube, depending on their molecular size. The characteristic speed, at which an ion moves, called ion’s drift velocity, is a distinct fingerprint that identifies the original substance. Vapor samples can also be collected and analyzed. Vapors are collected by drawing them into the instrument for analysis, where the same procedure as particle analysis is carried out. The only difference is in how the sample is introduced into the system. It was claimed that the detection limits of Ionscan was 50 to 350 pg for some common explosives, including plastic explosives [Eiceman and Karpas, 1993].

Often, the physical properties of what investigators are looking for will determine whether they collect particles or vapors. For example, most explosives do not give off enough vapors to be reliably detected with vapor sampling. Particle sampling, therefore, works best when sampling for explosives. Chemical warfare agents, on the other hand, have a large vapor presence, so vapor sampling is ideal when trying to confirm if a chemical warfare agent is in the air.

Recently developed GC-Ionscan [ornl.gov] is an another ion mobility spectrometry device, which is a fully transportable field screening instrument that combines the Ionscan's ease of use, speed of analysis and sensitivity with the additional separation capabilities of gas chromatography. The GC-Ionscan offers a dual analysis approach instrument. In Ionscan mode, samples can be rapidly pre-screened (qualitative) in 6-8 seconds by direct analysis. In GC-Ionscan mode, samples can be further confirmed in minutes to provide improved resolution and quantitative results.

Itemiser, EntryScan, and Vapor Tracer, patented by Sandia Research Laboratory and licensed by GE Ion Track [Parmeter et al., 2000], are three different detectors of trace amount of explosives and narcotics. The desktop Itemiser is able to detect trace amount

of both explosives and narcotics. A "sample trap" is swiped on the surface of any item suspected of being contaminated with traces of contraband and inserts it for automatic analysis. It is easy to operate, delivers fast and simultaneous detection of explosives and narcotics, lightweight, ergonomic, robust, and portable. EntryScan is a walk-through portal quickly screens people for contraband without physical contact and detects a wider range of explosives and narcotics with high sensitivity, as per the claim of GE Ion Trak. This device is considered as a complement to X-ray and metal detectors. A natural upward airflow around the body is generated to collect microscopic particles for analysis in the EntryScan. To ensure clean samples forced circulation system, such as a fan, is avoided in this system. Because forced air flow stirs up dust and other contaminants. According to the manufacturer, EntryScan has fewer moving parts, so it offers quieter operation, reduced weight and improved long-term reliability. Vapor Tracer, the handheld detector, sniffs vapor samples of contraband as well as analyze invisible particles collected in "sample traps" swiped over skin, baggage, vehicles, containers, tickets or ID cards. Swiping works well for detecting heroin, marijuana and PETN, while vapor analysis is more effective for dynamite, nitroglycerin and methamphetamine, claimed by the manufacturer.

It is noteworthy that the detection limits of several commercially available devices do vary by more than an order of magnitude as estimated in the literature [Steinfeld et al., 1998]. Fetterolf and coworkers [Fetterolf and Clark, 1993; Fetterolf et al., 1994] evaluated the Barringer Ionscan series of instruments [Ritchie et al., 1994] and observed 200-pg limits of detection for several of the common explosives. An RDX detection limit of approximately 20 pg using a PCP Model 110 was reported by Hallowell et al. (Hallowell et al., 1994). Using the same device Davies et al. [Davies et al., 1993] reported their calibration studies yielded 95% confidence limits on an observation of 5 pg RDX of ±14 pg. McGann et al (McGann et al., 1994) mentioned only a 115-pg detection

limit for cocaine while describing the application of the IonTrack Ion Trap Mobility Spectrometer to narcotics and explosives. Steiner et al. [Steiner et al., 2005] reported the detection of chemical warfare agent nerve simulant, di-Me methylphosphonate (DMMP), by coupled IMS with mass spectrometry (MS) in less than 12 ms.

1.3.4 Drug Detection

Ion mobility spectrometry is a very useful technique for detecting hidden contraband materials. Its high sensitivity, specificity, rapid response, and working characteristics under atmospheric pressure make it indispensable in drug detection technology. Karasek et al. [Karasek et al., 1976] first realized heroin and cocaine with their laboratory-model IMS directly coupled with mass spectrometer. They found the molecular ions (M^+), $(M.H_2)^+$, and $(M.CH_3CO_2)^+$ in heroin and $(M)^+$, $(M.C_6H_5CO_2)$+, and $(M.C_6H_5CO_2.CH_3CO_2)^+$ in cocaine in the positive ion mobility spectra. Matz et al. [Matz et al., 2001] used ion mobility spectrometry as a tool for the separation of opiate compounds e.g., normorphine, morphine, norcodeine, codeine, 6- monoacetyl morphine, 6- monoacetyl codeine, and heroin. Another abused class of drugs, benzodiazepines, were analyzed by Matz et al. [Matz et al., 2002] using electrospray ionization (ESI)-ion mobility spectrometry (IMS)- mass spectrometry (MS). Wu et al. [Wu et al., 2000] reported ionization and detection of illicit drugs, such as, amphetamine, methamphetamine, morphine, cocaine, heroin, etc. using IMS technology.

Lawrence and co-workers [Lawrence and Elial, 1985] performed field tests for drug detection in mail, luggage, and personnel with detachable sampling cartridge. Innocent letters were distinguished from that of with narcotics. They were also able to detect drugs in suitcase where the samples were close to the zipper, and hands and pockets of an individual with a full confidence as no false alarms were received from drug free items. Chauhan et al. [Chauhan et al., 1991] performed similar tests in letter

mails and cargo containers. Using IMS, they examined 339 letters out of which 4 were detected to carry drugs. Two false-positive results were obtained in this examination, however, one of which was found carrying a tarry morphine substance upon further investigation by Gas chromatography (GC)/ Mass spectrometry (MS). Their examination using IMS, for cocaine in containers, resulted 13 correct responses out of 18 containers with 5 false-negative responses. Verification of the content of some medicines sold over the counter was performed by Eiceman et al. [Eiceman et al., 1990] using IMS. After warming up the tablet or capsule slightly, the vapors were given off and checked by the hand-held IMS device and a spectra of constituents was obtained. It was then compared with the known one to confirm the contents mentioned in the prescription.

1.4 Miniature Ion Mobility Spectrometer

A recent trend of miniaturization of ion mobility spectrometer (as shown in Fig. 1.2) has attracted the researchers in this field due to several advantages in reducing the size of IMS devices. Miniature IMS devices are reduced in size, weight, and cost. Several modifications have taken place for improvements of miniaturized systems. The use of non-radioactive ion source, such as, a pulsed corona discharge source, and simple adsorptive scrubbing through gas diffusion for the cleaning of the drift system are among them [Baumbach and Eiceman, 1999].

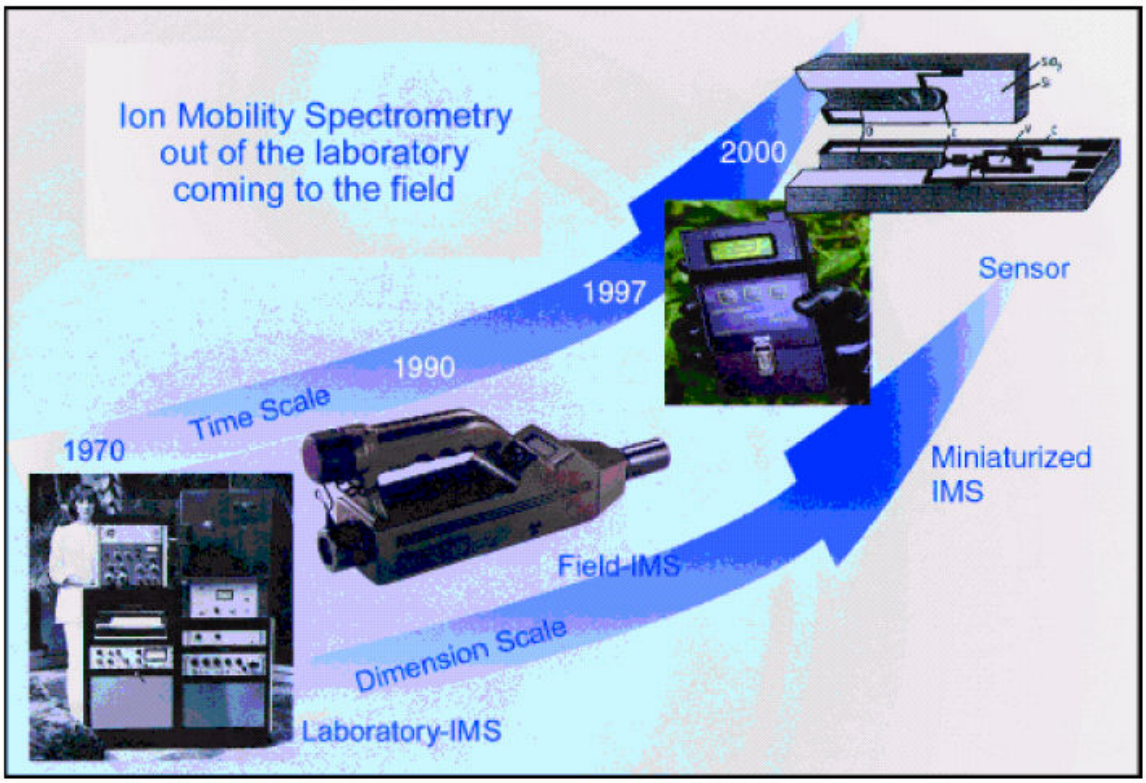

Fig. 1.2 Trend of miniaturization of ion mobility spectrometer [Courtesy: Ref. Baumbach and Eiceman, 1999].

In the 1970s IMS instruments were first introduced as desk-size units shown in Fig. 1.2. These chemical agent monitor (CAM) were used daily for years with little maintenance and repairing was relatively fast and convenient which proved them to be very high quality in engineering point of view. However, they showed little promise toward the eventual reduction in size [Baumbach and Eiceman, 1999]. With time technology for hand held IMS instrument was invented. As shown in Fig. 1.2**,** all utilities, data processing, drift tube control, and display of results are included in the hand-held unit. These instruments are able to display the analysis and results instantly to the user as the digital signal processing is made on board [Baumbach and Eiceman, 1999]. As an analytical instrument the CAM can be operated in hostile environment without failure.

During the Desert Storm in 1992, CAMs were extensively used as an agent monitoring device and demonstrated for further reduction in size [Baumbach and Eiceman, 1999]. The consequence of this demand is the mini-IMS system as shown in Fig. 1.2. The mini-IMS is a palm-size analyzer with analytical features that in some respects are advanced when compared to the CAM [Baumbach and Eiceman, 1999].

Miller and co-workers [Miller et al., 2000] first fabricated miniaturized field asymmetric ion mobility spectrometer (FAIMS) using Pyrex substrates and heavily boron doped silicon wafer. Silicon wafer of 500 μm thick was placed in between the two Pyrex substrates and determined the thickness of the drift tube. Titanium (40 nm) and Gold (120 nm) were deposited on the Pyrex substrates to form ion filter, a deflector electrode and a detector electrode. Patterning of Ti/Au electrode was performed by conventional lift off process using Shipley 1822 photoresist. Once the electrodes were formed silicon wafers were diced into strips and bonded with Pyrex by the anodic bonding process (electric field ~ 1000 V, and temperature 350^0C). A photo-ionization source (10.6 eV photo discharge lamp, λ = 116.5 nm) was connected to the device by drilling holes into the top Pyrex to provide a means for the photons to enter the ionization region. Detection of benzene, acetone and toluene ions was demonstrated by this device. And for the first time, the transportation of both positive and negative ions simultaneously through the FAIMS drift tube was demonstrated using this miniaturized device.

The miniaturized atmospheric pressure radio frequency (RF) ion mobility spectrometer (IMS) developed by Eiceman et al. [Eiceman et al., 2000] worked as an ion filter for atmospheric pressure chemical ionization (APCI) mass spectrometer. This ion filter, positioned between the ion source and the flange of the mass spectrometer, worked as an ion separator before the ions get into the mass spectrometer. The drift tube of the miniaturized RF-IMS device was fabricated from two Pyrex substrate separated by a 500

µm thick silicon wafers. The drift tube was 30 mm long, 10 mm wide and 2 mm deep. Gold electrodes were deposited on both the top and bottom substrates. Nitrogen or air was used as drift gases at a flow rate of 2 L/min to sweep the ions out of the drift tube. When ions passed through the drift region an RF field of 2 MHz frequency was applied between the top and bottom electrodes. The RF field had an asymmetric waveform with high (20,000 V/cm) and low (-1000 V/cm) and was superimposed by a DC electric field (compensation voltage) of – 400 to + 400 V/cm. The compensation voltage was adjusted to select and pass ions through the filter into the mass spectrometer. A schematic has been shown in Fig. 1.3 which shows selected ions deflect and pass through the pinhole into the vacuum flange of the mass spectrometer. They used binary mixtures of volatile organic compounds to demonstrate continuous monitoring with a photo-discharge lamp ion source and ion pre-separation before mass analysis.

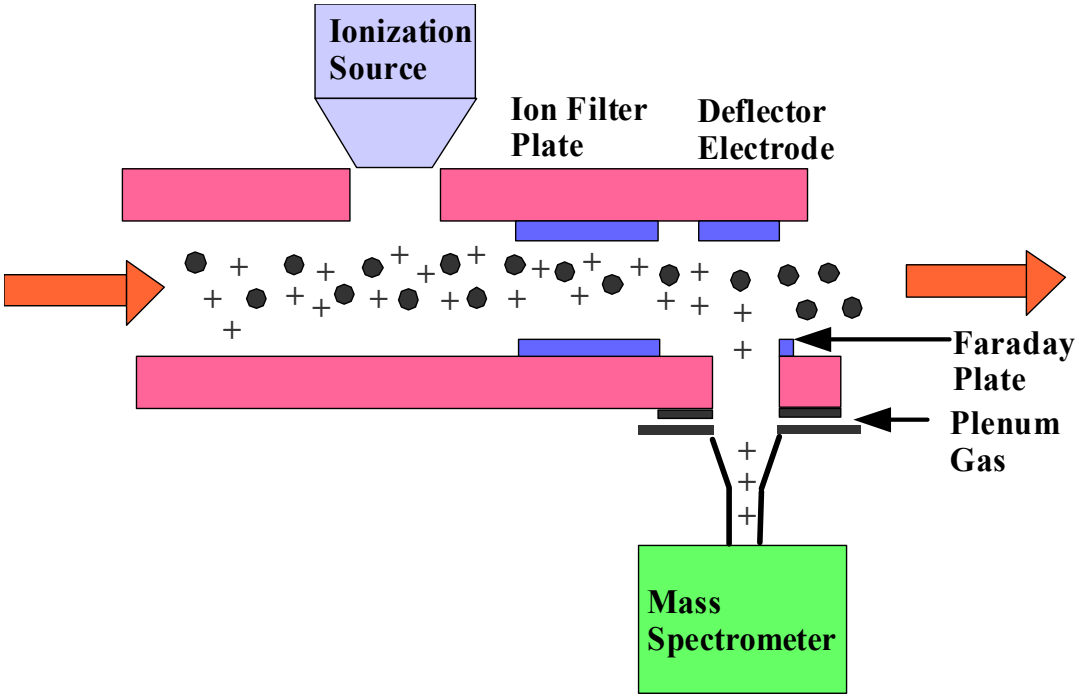

Fig. 1.3 Schematic of micro-machined drift tube as an ion filter for APCI-MS [Courtesy: adapted from Eiceman et al., 2000].

Xu et al. [Xu et al., 2000] presented the effects of Coulomb repulsion on pulse broadening in miniature ion mobility spectrometers at atmospheric pressure. Their miniature IMS device was 35 mm in length having a 1.7-mm-diameter drift channel. There were 25 metal electrodes stacked in the channel and are separated by insulator spacers. The electrodes were made of oxygen-free high density copper (OFHC) with a thickness of 0.33 mm. The insulator spacers were made of Macor with an inner diameter of 3 mm, outer diameter of 15.7 mm, and thickness of 1.1 mm. Total 24 miniature resistors were connected between the electrodes to form a voltage divider. Each resistor had 1 MΩ with 1% uncertainty. To apply the drift voltage along the channel, a power supply was connected to end electrodes and the voltage was distributed to sequential electrodes through these resistors. They observed linear decrease in potential along the channel which indicated a nearly homogeneous electrostatic field produced in the drift region. The electrode next to the detector plate was ac-grounded through a capacitor so the electric current due to ion movement would not be coupled to the detector. For their device they used a frequency-quadrupled Nd: YAG laser for ionization of samples of NO, O_2, and methyl iodide (CH_3I). N_2 was used as the drift gas.

Xu et al. [Xu et al., 2003] also demonstrated the pulsed corona discharge ionization in gas phase for miniaturized ion mobility spectrometer. In this experiment the drift channel was 2.5 mm in diameter and 47 mm in effective length. The drift channel was comprised of 10 stacked oxygen free high-density copper (OFHC) electrode with 1.2 mm thick and separated by Teflon spacers. Nine Miniature resistors of 2 MΩ each were connected between the electrodes to form a voltage divider. The rest of the setup was as above. Ions were generated by a combination of both pulsed potential and dc potential. Ionization of air was performed at atmospheric pressure and room temperature. The drift gas N_2 was fed from the detector end of the IMS channel with a flow rate of 20 standard cubic centimeter per minute (sccm). The authors concluded from this experiment that the

miniature IMS with pulsed corona ionization could be interfaced with miniature gas chromatograph or a miniature ion trap mass spectrometer.

1.5 Motivation

1.5.1 Motivation for Miniaturized Ion Detection Device in Liquid Phase

The goal of this research is to develop a microchip for ionization and detection of ions in liquid phase, which are two major parts of ion mobility spectrometry (IMS). Moreover, integration of the ionization source with the drift system is very crucial as well as extremely essential for the miniaturization of such devices in field applications. This is another very important objective of this research. The integration of the ionization source simplifies the components required to build and assemble the IMS setup. The total microchip should be polymer based.

It is noteworthy that gas phase IMS is being used successfully for various monitoring and detection purposes related to public safety, however, the separation efficiency of gas phase IMS suffers as the instrument is scaled down. This problem can be solved by substituting the gas medium with a liquid medium due to the fact that ions diffuse 2-3000 times slower in liquids than in gases [Hill et. al., 2005]. Therefore, a micro-scale liquid phase IMS can provide real-time analysis with high separation efficiency. Keeping this in mind we targeted to achieve above-mentioned goal as the first step of our stand alone miniaturized device.

1.5.2 Reason to Introduce Poly-di-methyl-siloxane

Typical laboratory-scale gas phase IMS has a stacked ring design, where circular ring electrodes are stacked together and separated by insulator rings. However, in micro-scale it is completely impossible to integrate the electrodes in the device. Poly-di-

methylsiloxane (PDMS) based microchip using soft lithography would be a better solution of this problem. Biocompatibility, reproducibility, electrically non-conductivity, and non-toxicity would make PDMS based micro device prospective for the detection of hazardous molecules and explosives. Not only that our developed techniques to integrate electrodes, detectors and the ionization source on the polymeric chip have provided an enormous thrust for this research. PDMS based microchips are also easy to fabricate, and inexpensive compared to the traditional stacked ring design. Portability of this micro device will enable it to become a ubiquitous detection device.

CHAPTER TWO

FABRICATION OF NOZZLE INTEGRATED MICROCHANNEL

2.1 Introduction

Following the trend of miniaturization, the development of microfluidic devices has been playing a significant role in recent years, especially in biological and environmental research fields. The main benefits of performing experiments in microfluidic device are the minimal uses of sample or reagent(s), reduction in analysis time, increase in resolution in bio-separations, low thermal dispersion of sample, etc. In the early 1990s, microfluidic devices were first fabricated in silicon wafer using micromachining technique (photolithography and etching) adapted from the microelectronics industry. Silicon microfluidic chip not only hinders the optical detection of bio-analytical processes in it, but is also very expensive even after batch processing. Later researchers chose optically transparent glass [Harrison et al., 1993] or quartz [Jacobson et al., 1995] as a microfluidic platform. However, devices fabricated with glass or quartz cannot be reused if they are clogged by precipitation of chemicals. In the last couple of years, polymeric based materials, such as poly-di-methyl-siloxane (PDMS), polymethyl-methacrylate, poly-carbonate, and teflon have received more attention as device materials to counteract the above-mentioned disadvantages of Si-wafer, glass, and quartz [Chovan and Guttman, 2002]. Microfluidic devices made of polymeric material can be mass-fabricated using injection molding, embossing, imprinting, laser ablation, or soft lithography [Becker and Locascio, 2002].

Among available polymeric materials, elastomeric PDMS is highly desirable in microfluidic applications for its characteristic of rapid prototyping with high fidelity using soft lithography technique [McDonald and Whitesides, 2002]. Some of the other advantages of using PDMS are: (i) it is optically transparent down to 280 nm so it can be

used for a number of confirmatory detection systems (UV/vis absorbance and fluorescence); (ii) it can be bonded to itself or other materials both reversibly and irreversibly depending on the system requirements; (iii) it is non-toxic and it works as perfect insulator; and (iv) it's surface chemistry can be controlled favorably for a number of bio-analytical operations, such as electrokinetic pumping, DNA separation, on-chip isoelectric focusing, etc. Due to the above mentioned advantages, PDMS based microfluidic devices are used for protein, cell and DNA separation and pre-concentration, electrokinetic pumping, micro-mixing, electro-spray ionization mass spectrometry, and fuel cell.

Researchers are now concentrating on highly integrated systems to use the microfluidic devices for chemical synthesis and analysis for lab-on-a-chip applications. Because true lab-on-a-chip devices offer the possibility of reducing cost by integrating processes that would otherwise require a suite of instruments and several manual manipulations in which human error and contamination can be introduced [Figeys and Pinto, 2000]. Hasselbrink et al. [Hasselbrink et al., 2002] created micropistons with Teflon-like non-stick polymer formulation inside the microfluidic channels (in glass chip with 25μm deep and the width of the channel contracts from 150μm to 50μm) using laser polymerization. The channel was completely filled with a mixture of monomer, solvent, and initiator. The typical formulations published in that paper was: (monomers) 1:1 trifluoroethyl acrylate/ 1,3-butanediol diacrylate (50-80%); (solvents) methoxyethanol/ 1,4-dioxane/ 5 mM TRIS buffer (total 20-50%); and (photoinitiator) 2,2′-azobisisobutyronitrile 0.5% (w/w). The mixture was then exposed to 355-nm light from a Nd:YAG laser (1 (mJ cm^2)/pulse, 10 Hz) through a chrome-on-quartz mask for 30-75 sec to initiate polymerization and cross-linking. Unwanted monomer was flushed away with organic solvent (via alternate conduits in the microfluidic system), while the moving part was held captive by geometric constrictions within the channel.

Although a number of UV sources can initiate photopolymerization, a laser confers higher resolution photodefinition of the part. Adams et al. [Adams et al., 2005] integrated two channels of different heights to develop PDMS based microfluidic diode. One of the channels was 11 microns high and 50 microns wide and the other one was either 24 microns, or 33 microns, or 42 microns high and 100 microns wide. Microchem SU8 2010 photoresist was used to pattern 11 microns high channel and SU8 2015 for the other channel. The orifice width at the intersection of the two channels was 25 microns.

We have introduced a nozzle of 12 μm deep and 50 μm wide at the tip in the ion mobility spectrometry system in considering that the nozzle will help ionization of the liquid and guide the ions toward the center line of the 400μm deep drift channel.

2.2 Microfabrication Technique

Fig. 2.1 shows the fabrication sequence to form PDMS microchannel. In this section, fabrication techniques are described for the nozzle and the 200 μm deep channels. The relevant parameters for 10μm and 50 μm deep channels are shown in Table 2.1. PDMS microchannels were fabricated using standard photolithography and replica molding techniques.

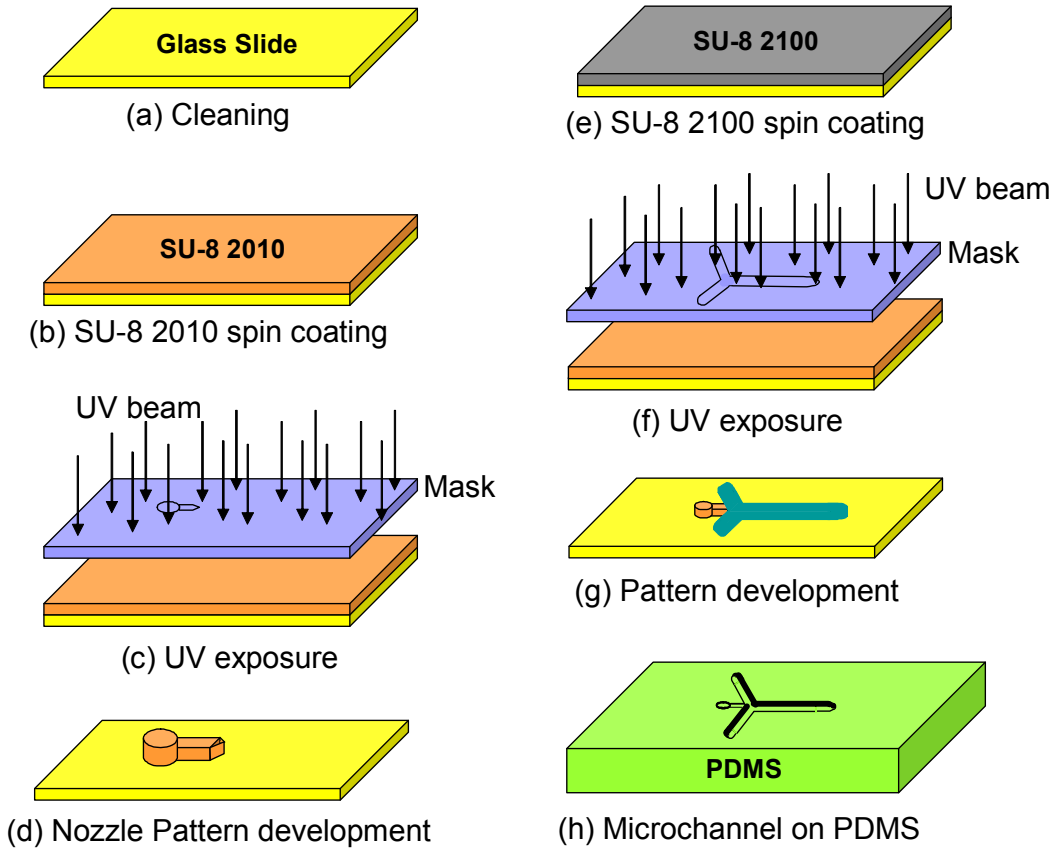

Fig. 2.1 Schematic view of microfabrication techniques to develop nozzle integrated microfluidic channel ((a)-(h)).

Table 2.1 Fabrication protocol used to form microchannels of different depths on PDMS

	10-μm-deep channel	50-μm-deep channel	200-μm-deep channel
Photoresist	AZ P4620	SU-8 2025	SU-8 2100
Substrate	Glass	Glass	Glass
Spin (rpm)	2000	1750	1550
Pre-bake (^{0}C)	N/A	65	65
Soft-bake (^{0}C)	80	95	95
Expose (mJ/cm^2)	290	380	650
Post-bake (^{0}C)	110	95	50
Hard-bake (^{0}C)	N/A	150	150
Develop (sec)	60	150	550

2.2.1 Nozzle fabrication

The microscope glass slide onto which the pattern was developed was cleaned with acetone, isopropyl alcohol and deionized water. In photolithography (fig. 2.1 (a)-(c)), SU-8 (MicroChem SU-8 2010) was spun (P-6000 Spin Coater, Specialty Coating Systems Inc., IN) onto the glass slide at 500 rpm for 13 sec and then 3000 rpm for 34 sec. In pre-baking the photoresist coated glass slide was heated on a hot plate (Digital Hot Plate/ Stirrer, Series 04644, Cole Parmer) at 65°C for 2 min, while in soft-baking the photoresist was heated in an oven (Thelco, Model 19, Precision Scientific Company, IL) at 95°C for 6 min. The photoresist was then exposed to near ultraviolet light (365 nm) at 150 mJ/cm^2 using a mask aligner (Hybralign, Series 500, Optical Associates Inc., CA)

through direct contact with a patterned mask that contains the desired shape of the microfluidic nozzle. The ultraviolet radiation causes the negative resist to become polymerized, which makes it more difficult to dissolve. Next, the glass slide was post-baked on a hot plate at 65^0C for 2 min and 95°C for 5 min. Finally, the photoresist was developed (fig. 2.1 (d)) with commercially available SU-8 developer (MicroChem Corp., MA). The developer solution removed only the unexposed portions of the photoresist, and the negative resist remained on the glass slide wherever it was exposed. Once the nozzle pattern was developed, the channel was ready for fabrication.

2.2.2 Channel fabrication

SU-8 (MicroChem SU-8 2100) was spun coated (fig. 2.1 (e)) onto the glass slide (at 1550 rpm) having the pattern of nozzle on it and baked (both pre-bake and soft-bake). This allowed to reach the desired thickness of 200 µm. Pre-baking of the photoresist was taken place on the hot plate at 65°C for 7 min, and soft-baking in the oven at 95°C for 120 min. The photoresist was exposed (fig. 2.1 (f)) to near UV light (365 nm) at 650 mJ/cm^2 to have the desired shape of the microfluidic channel at the tip of the nozzle pattern. The glass slide was post-baked at 50^0C for 60 min. Finally, the photoresist was developed (fig. 2.1 (g)) with SU-8 developer. Once the pattern of the nozzle and the microchannel were developed, two components of PDMS (pre-polymer and curing agent) (Sylgard 184, Silicone Elastomer Kit, Dow Corning Corporation, MI) [Dowcroning's website] were mixed at 10:1 ratio (by volume) and degassed until no air bubbles remained in the mixture. The liquid PDMS was then poured into the mold to a height of about 5 mm. The PDMS was polymerized by curing in an oven for 3 hr at 80°C. At the end of the curing process, the solidified PDMS layers were peeled off from the mold (fig. 2.1 (h)). The resultant slab was the bottom layer of our microfluidic channel. For the top layer of the channel, an identical procedure was followed, except the nozzle.

2.3 Discussion

In this chapter, nozzle integrated microfluidic channel fabrication technique has been explained. Ion spraying and guiding the ions through the center line of the drift channel play a very important role in ion mobility spectrometry. Integration of the nozzle makes those processes easier.

CHAPTER THREE

PATTERNING OF PLATINUM MICROELECTRODES IN POLYMERIC MICROFLUIDIC CHIP

3.1 Introduction

Miniaturized electrodes are one of the most important components of "lab-on-a-chip" devices for separation, pumping, sensing, and other bio-analyses. In microfluidic based chemical and bio-analytical operations, platinum electrodes are preferred to minimize the interaction with chemicals or biomolecules due to their chemical inertness. Although microfabrication techniques for patterning integrated platinum microelectrodes on Si-wafer, quartz or glass substrate are available, no techniques have been reported so far for depositing platinum electrodes on soft polymeric surfaces. In this study, a novel fabrication scheme for forming integrated microelectrodes in a poly-di-methyl-siloxane (PDMS) microchip is described. The electrode fabrication technique consists of photolithography, thermal processing, sequential sputtering of titanium and platinum and stripping off photoresist, while soft-lithography is used to form the microfluidic channels on PDMS. This fabrication technique allows to pattern microelectrodes in PDMS microchannels, and can be used for both low and high aspect ratio channels. This approach facilitates precise positioning of the electrodes with micron-sized gap between them without using hazardous chemicals. Platinum electrodes, formed on the PDMS channel surface, demonstrate very good interfacial adhesion with the substrate due to the use of a very thin titanium layer between the platinum and PDMS.

Using Pt wire, electrokinetic focusing was performed in the glass microchips developed by Jacobson and Ramsey [Jacobson and Ramsey, 1997]. For DNA sequencing in channels in fused-silica wafers, Schmalzing et al. [Schmalzing et al., 1998] used platinum wire electrodes in four fluid reservoirs to provide high voltage. Burns et al.

[Burns et al., 1998] placed Ti/Pt electrodes (20 nm/30 nm) (Pt was the working electrode) on top of the p-xylylene layer for electrophoresis. Webster et al. [Webster et al., 2001] developed monolithic capillary electrophoresis system on silicon substrate in which 0.1μm thick gold electrodes were patterned on the parylene layer (which was deposited on top of SiO_2) by liftoff. Gottschlich et al. [Gottschlich et al., 2001] devised a two-dimensional separation system for electrochromatography and capillary electrophoresis. They used platinum wires at the reservoirs to apply high voltage. A 200 nm thick Pt-layer was deposited by electron beam evaporation on the oxidized Si wafer by Brahmasandra et al. [Brahmasandra et al., 2001] in their DNA separation system. Alarie et al. [Alarie et al., 2001] reported glass microchip, for pinched injection strategy in electrophoretic injection bias, developed by standard photolithographic technique and wet etching. They inserted the Pt-electrodes into the fluid reservoirs to apply high voltages. Hong et al. [Hong et al., 2001] developed a PDMS based microchip for capillary gel electrophoresis to separate DNA molecules of different sizes. They introduced reservoirs and electrodes by drilling the PMMA plate, and microchannel was on the PDMS layer. Chiou et al. [Chiou et al., 2002] developed PDMS based micro device for electrospray ionization mass spectrometry (ESI-MS) for protein identification where they introduced Pt wires as electrodes while casting the PDMS to drive the sample by electro-osmotic forces. Sanders et al. [Sanders et al., 2002] embedded Pt electrodes into PDMS prior to the curing process while developing microchip for electrophoretic separations. Fu et al. [Fu et al., 2003] proposed a moving electric field technique, where the electrodes were laid down onto the glass slides for DNA fragment separation within a low voltage driven capillary electrophoresis (CE) chip. For immunosensing biochips, Ko et al. [Ko et al., 2003] deposited Cr (20 nm) and Au (200 nm) layers consecutively onto the embossed PMMA substrate by an E-beam evaporator. They used 100-μm-thick shadow mask, which was laser cut, as the pattern of gold electrodes prior to the Cr/Au deposition. Mitrovski et al. [Mitrovski et al., 2004] fabricated a microfluidic H_2-O_2 fuel cell

comprising of Pt-electrodes deposited on quartz and the remaining part of the device was of PDMS. Pal et al. [Pal et al., 2005] developed a microfluidic device for genetic analyses which comprised of Ti/Pt layers (30 nm/100 nm) as heater on oxidized silicon wafer (<100>).

PDMS can be bonded with a number of metals, such as titanium (Ti), titanium-tungsten (TiW), gold (Au), platinum (Pt), etc. This specific bonding characteristic enables deposition of metal(s) onto PDMS surface. However, the flexibility of PDMS layer is the major bottleneck for precise patterning of electrodes on PDMS surface, especially for deep microchannel. This problem can be eliminated by bonding the PDMS channel with a glass, acrylic, or Si substrate. Gold microelectrodes can easily be patterned on flat PDMS surface because of the availability of the gold etchant. Lee et al. [Lee et al., 2005] deposited titanium (1 nm)/ gold (20 nm) electrodes on PDMS surface by using electron beam evaporator to demonstrate soft-contact optical lithography. However, chemically active gold reacts with sample and/or organic compounds used in bioanalytical processes, and obstructs the flow inside the channel by forming bubbles. In some instances, gold electrodes disappear from the microchannel surfaces due to corrosion. Hence, chemically inert platinum is preferred as an electrode material for microfluidic based sensing, separation, etc. There exist a number of studies where platinum electrodes were formed on different substrates, such as p-xylylene [Burns et al., 1998], silicon wafer [Brahmasandra et al., 2001; Pal et al., 2005], quartz [Mitrovski et al., 2004] and glass [Hiratsuka et al., 2001]. Formation of platinum electrodes on such hard surface consists of three fundamental steps. First, a pattern is formed on the hard substrate using photolithography technique. This is followed by the deposition of platinum using evaporation [Burns et al., 1998] or electron beam deposition [Brahmasandra et al., 2001]. Finally, the substrate is kept in acetone for 15-30 minutes to take-off unwanted metals with photoresist leaving the patterned electrodes on the

substrate [Pal et al., 2005]. But the above mentioned technique is not appropriate for forming platinum microelectrodes on PDMS microchannel.

To our knowledge, no previous studies addressed the direct deposition of platinum on flexible PDMS surface or around a microchannel. There are a number of challenges in forming platinum microelectrodes on PMDS. First, it is almost impossible to etch platinum completely. A Pt- enchant (from Transene Company, Inc., Danvers Industrial Park, Danvers, MA) was commercially available, however, due to inconsistent results this product was discontinued recently. Aqua regia, a mixture of nitric and hydrochloric acids, could still be used to wet etch platinum, but it is not advisable to use that chemical because of potential health hazards. Second, traditional lift-off process of platinum does not work for PDMS, especially for deep microchannel. So, in this communication we describe a microfabrication technique of platinum electrodes on the PDMS microchannel surfaces using a combination of thermal processing and strip-off techniques. This method can easily be implemented in clean rooms without using hazardous chemicals. This fabrication process includes photolithography, thermal processing, sequential electrodes sputtering, and stripping off photoresist. In this study, the microchannel height was varied from 10 to 400 microns, while the electrode thickness was kept below 350 nm. The length and width of electrodes were varied from case to case.

3.2 Microfabrication Technique

Our next step was to form microelectrodes on PDMS surface. Fig. 3.1 shows the fabrication sequence to form patterned platinum microelectrodes around the channel.

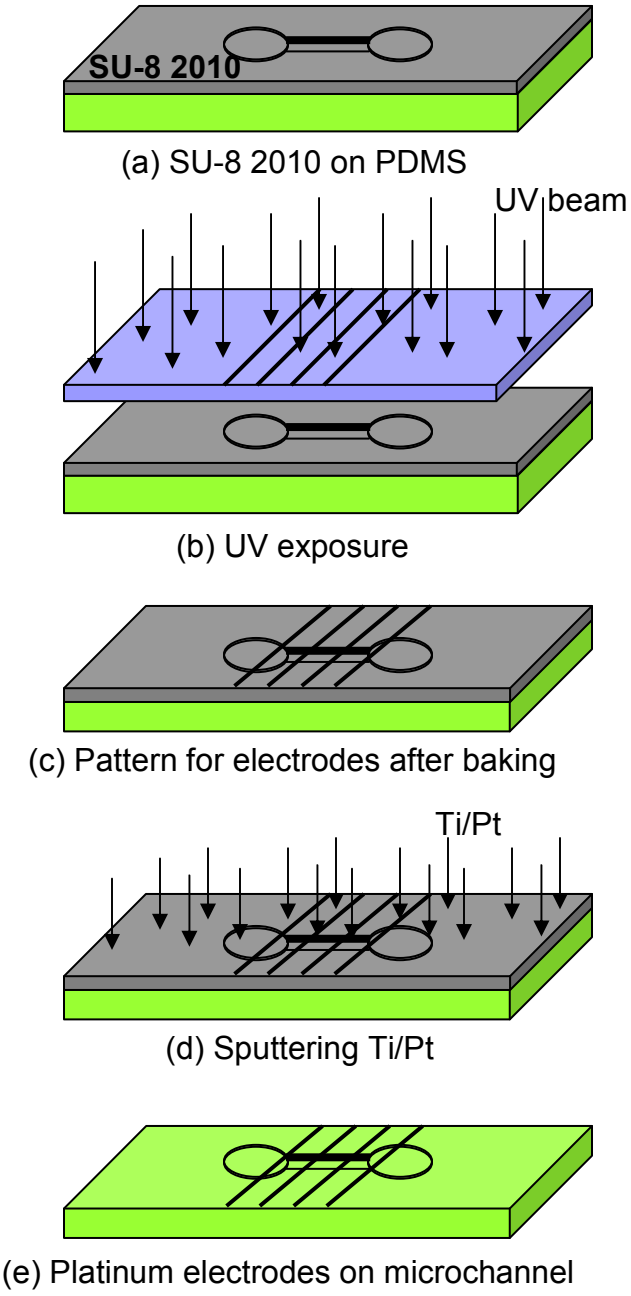

Fig. 3.1 Schematic view of microfabrication techniques to form patterned electrodes around the PDMS microchannel ((a) – (e)).

In this study, we developed a technique to pattern platinum in PDMS microchannel. To accomplish this, PDMS surfaces with microchannel structures were

spin coated (at 1000 rpm for 19 sec) with SU-8 2010 (fig. 3.1 (a)), and pre-baked and soft-baked at 65^0C and 95^0C, respectively. This resulted in a photoresist layer of about 30 μm thick. Then, the photoresist was exposed (fig. 3.1 (b)) to near ultraviolet radiation at 210 mJ/cm^2 and developed for 60 sec in the SU-8 developer (MicroChem Corp., MA). The bonding strength of PDMS and SU-8 is generally poor due to the low surface energy of PDMS. This particular property is helpful for stripping-off SU-8 from the PDMS surface. The photoresist coated PDMS channel was then baked (fig. 3.1 (c)) at 115^0C for 150 sec. This hardened the photoresist and aided in the lift-off process. The PDMS layer with the developed pattern was then cleaned with RF plasma in presence of oxygen gas (Plasma Etcher PE 2000, South Bay Technology Inc., San Clemente, CA). This temporarily activated the exposed part of the PDMS and provided very good adhesion property with the metal. The patterned PDMS channel was then loaded into the sputtering machine (Edwards Auto 306, BOC Edwards, MA). A titanium thin film (30 nm thick) was deposited at 0.4 A for 195 sec followed by a platinum layer (320 nm thick) at a dc power of 60 W for 30 min (fig. 3.1 (d)). A titanium thin film was used as an adhesion layer for platinum electrodes because the bonding strength between the PDMS and platinum is normally very weak. In microfluidic applications, usually a very high pressure is used to load sample and reagents. Therefore, a good bonding strength is necessary for integrated electrodes on the microchannel surface.

The sputtering of the metals (Ti/Pt) on the photoresist caused increased brittleness of the photoresist. This facilitated easy removal of metal coated photoresist from the PDMS surface. Using this procedure, one can avoid the use of hazardous chemicals for platinum etching. The PDMS channels patterned with platinum electrodes were then cleaned with acetone, isopropyl alcohol, and DI water (fig. 3.1 (e)). For permanent bonding of top and bottom layers, both layers were cleaned by oxygen RF plasma (PDC-32G, Harrick Scientific Co., NY) for 20 sec prior to the bonding. Oxygen plasma

treatment renders the PDMS surface hydrophilic. This also facilitates easy loading of sample due to the replacement of CH_3-groups with OH-groups.

3.3 Topography of Embedded Microelectrodes

Scanning electron microscopy (SEM, Sirion200, FEI Company, OR) pictures of the electrodes embedded in channels of different depths are shown in Fig. 3.2. These pictures were taken at different magnifications ranging from 33x to 2000x. Fig. 3.2 (a) illustrates platinum electrodes patterned on a flat PDMS surface. This was observed at 80x magnification.

In microfluidic devices, the surface roughness of electrodes is one of the most important concerns, as the platinum embedded microchannel will be bonded to an identical PDMS layer. Fig. 3.2 (b) shows the surface quality of platinum electrode shown in Fig. 3.2 (a). This picture was taken using SEM with 2000x magnification. Though there seem to be very tiny bumps of couple of nano meters in size (in fig. 3.2 (b)), the overall electrode surface is highly smooth. No seeping of liquid through the intersection was observed, when the platinum embedded surface was bonded with a PDMS microchannel and benzene was allowed to flow through the microchannel. Platinum electrodes were also successfully patterned in PDMS microchannels of different depths. Figure 3.2 (c) - (e) show the Pt-electrodes around 10-, 50-, and 200- μm-deep channels. These images also indicate that the side surface of the electrode is very smooth and vertical.

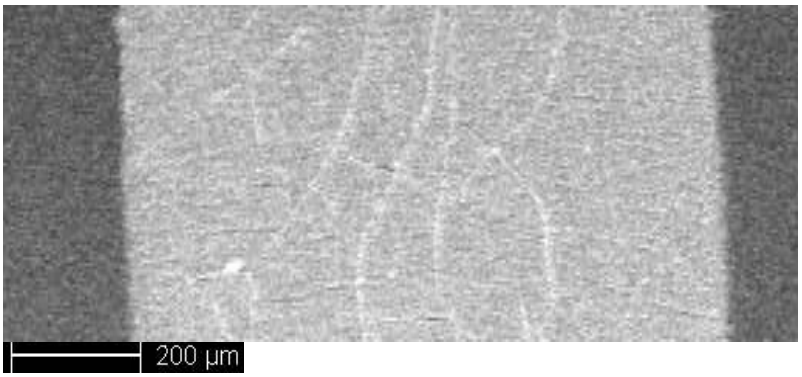

(a)

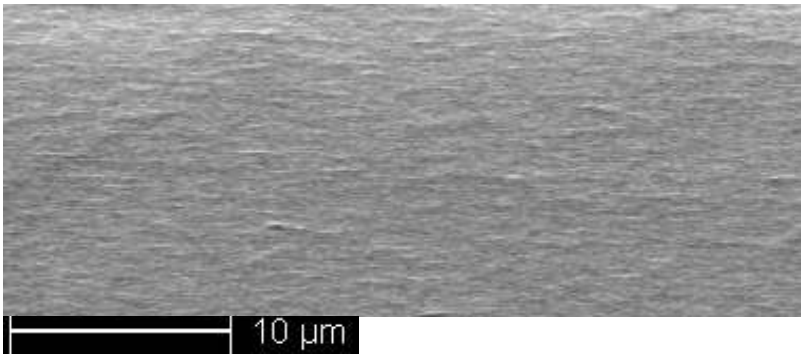

(b)

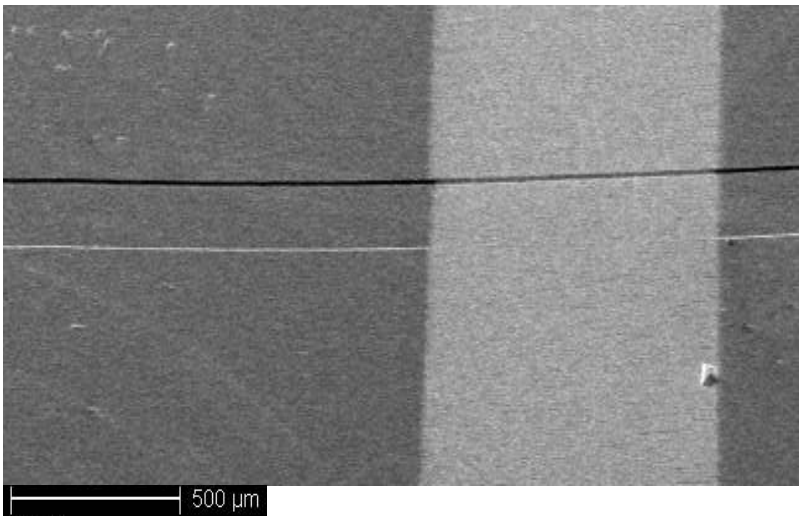

(c)

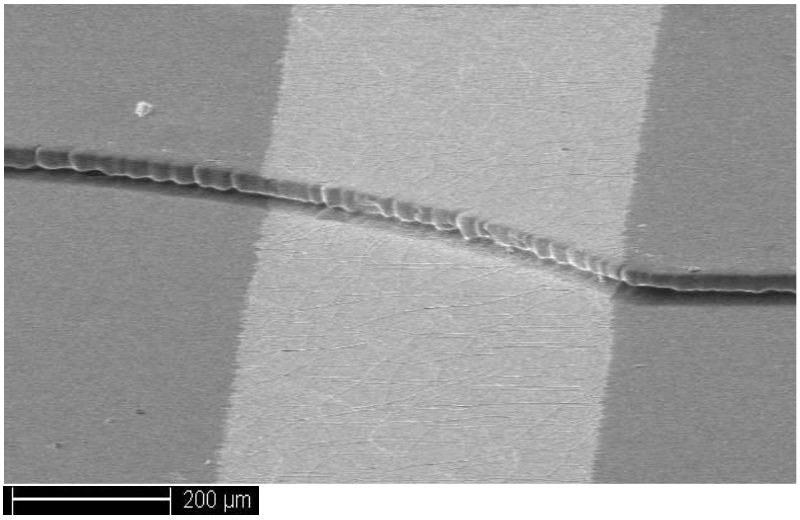

(d)

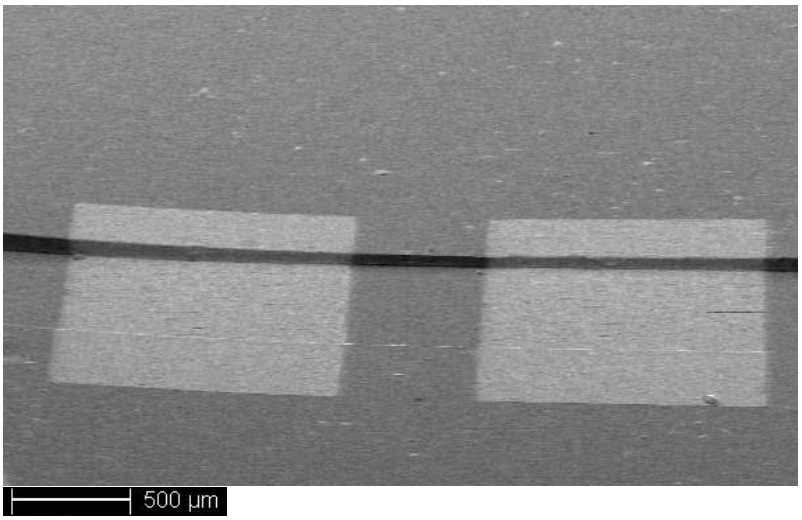

(e)

Fig. 3.2 SEM images of patterned platinum electrodes on flat PDMS surface (a) 80x magnification (b) 2000x magnification. SEM images of patterned electrodes in PDMS microchannel for (c) 10 µm (52x mag.), (d) 50 µm (119x mag.) and (e) 200 µm (33x mag.) channel depth.

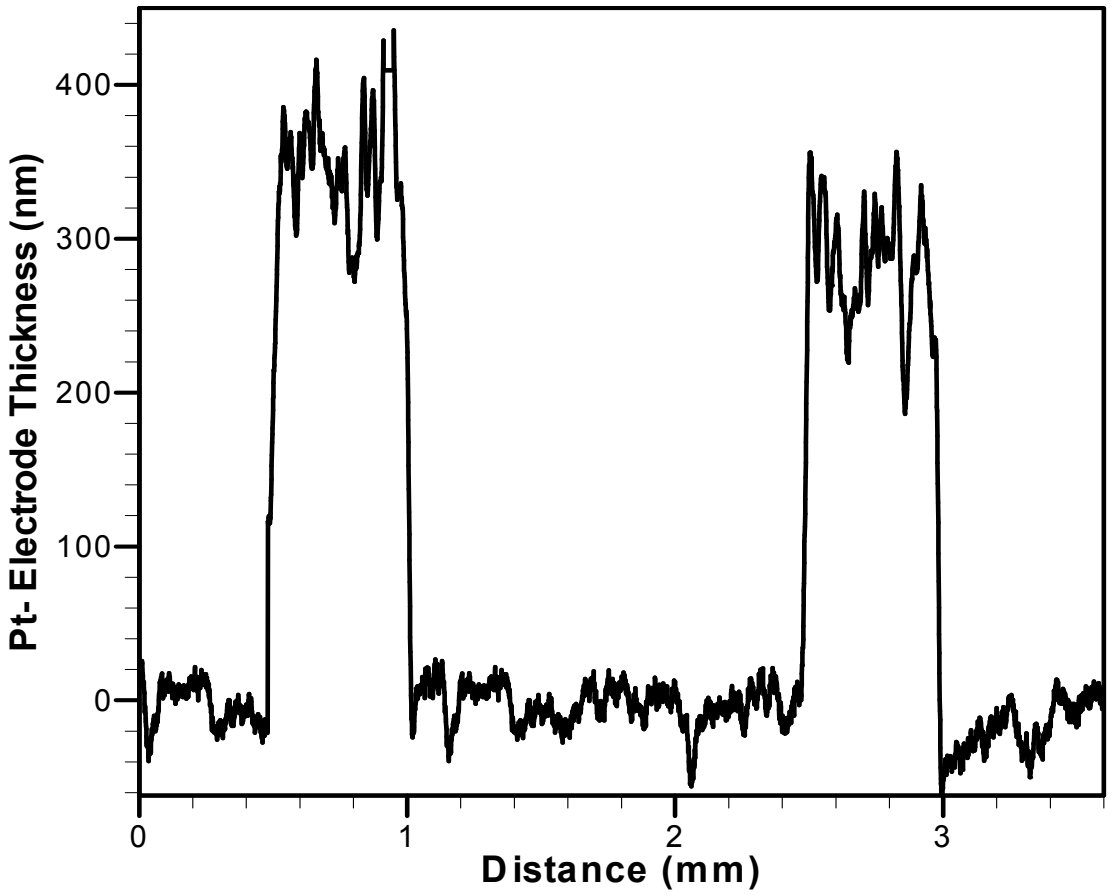

Fig. 3.3 Quantitative measurement of deposited platinum thickness on PDMS. The depth of the electrode is measured as 300-400nm. The surface roughness of PDMS is less than 50 nm, while the surface roughness of sputtered electrodes is varied between -50 nm and +50 nm. This measurement was done by a profilometer (SPN Technology, Inc., CA) which provides quantitative values with atomic resolution.

A quantitative profile of platinum electrodes on the PDMS surface has been shown in Fig. 3.3. This measurement was done by a profilometer (SPN Technology, Inc., CA) which provides quantitative values with atomic resolution. From this figure, the depth of the electrode can be measured as 300-400 nm. The thickness of the electrode differs slightly from our designed value. This error could be due to inconsistent sputtering rate over time since the sputtering process is machine dependent. From Fig. 3.3, it is clear that the surface roughness of PDMS is less than 50 nm, while the surface roughness of sputtered electrodes is varied between -50 nm and +50 nm. Surface roughness of PDMS mainly originates from the roughness of the microscope glass slide (as shown in fig. 3.4) used in photolithography. The average surface roughness of the glass slide is observed as ± 50 nm. This roughness is introduced into the PDMS surface and the channel in it and causes the roughness of the sputtered electrodes. However, the surface condition could be improved by using a high-quality silicon wafer during the photoresist patterning and molding processes. The relatively high surface roughness on the patterned platinum electrodes could be due to both surface coarseness of PDMS and the uncertainty involved in the sputtering process. Surface roughness due to sputtering process can be reduced by achieving high vacuum in the sputtering chamber.

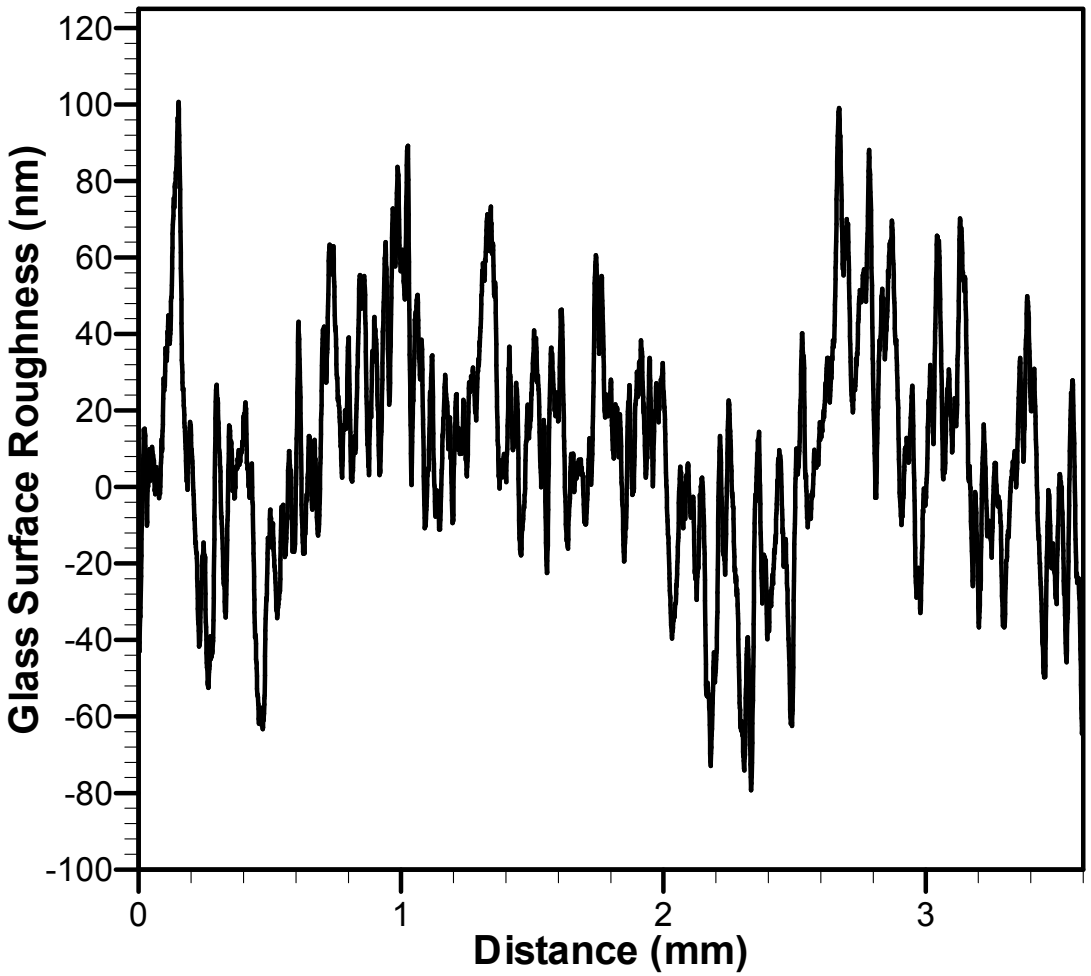

Fig. 3.4 Surface roughness of a commercially available microscopic glass slide. The average surface roughness of the glass slide is observed as ± 50 nm. This roughness is introduced into the PDMS surface and the channel in it and causes the roughness of the sputtered electrodes. This measurement was also performed by a profilometer from SPN Technology, Inc., CA.

3.4 Current Check using Embedded Microelectrodes

This section demonstrates the sensing ability of integrated microelectrodes in a PDMS microchip. Fig. 3.5 (a) shows the photograph of a PDMS microchip with

embedded platinum electrodes. The electrodes are embedded in the microchannel (200-μm-deep) and extended outside for electrical connections. Here electrode # 0 is connected to a high voltage power supply (6110A DC Power Supply, Hewlett Packard, 0-3000 V, 0- 6 mA) to ionize the sample. Electrodes # 1 to # 5 are connected to another high voltage power supply (6516A DC Power Supply, Hewlett Packard, 0- 3000 V, 0- 6 mA) to maintain a uniform electric field along the channel, while electrode # 6 (sensor hereafter) is hooked up with a current amplifier (427 Current Amplifier, Keithley Instruments, OH). The current detected by the sensor is amplified with a gain of 10^6 volt/ amp. The voltage signal is then received and monitored by a digital multimeter (Fluke 187 RMS Multimeter, Fluke Corporation, WA). The ion current, therefore, detected by the sensor can be obtained by dividing the output voltage with amplifier gain.

In this study, the current monitoring experiments were performed at a constant flow rate. Benzene, a non-polar liquid, and methyl alcohol (CH_3OH) and water (90:10) were used as the drift liquid and sample respectively for this experiment. A syringe pump was connected to the end of the channel via a capillary to maintain a constant flow rate of 5 μL/min of benzene in the microchannel. Sample was fed into the nozzle at a flow rate of 0.1 μL/min using another syringe pump. Currents recorded by the sensor are presented in Fig. 3.5 (b) for different electrodispersion ionization voltages. When there was no electrospray ionization potential, a negligible amount of current of about 0.02 nA was detected. This negligible amount of current was probably due to the electronic noise of power supply, amplifier, and other electrical devices. As the ionization potential was raised to 0.5 kV the sample ionized. This is depicted in Fig. 3.5 (b) by an ion current of 0.15 nA. With increase in electrodispersion voltage, more ion current was detected. The maximum voltage applied in this study was much less than the dielectric strength (100 kV/mm) of benzene to avoid leakage current between electrodes. The smooth current

responses due to the voltage change confirm the integrity and continuity of the platinum electrodes both inside and outside of the channel.

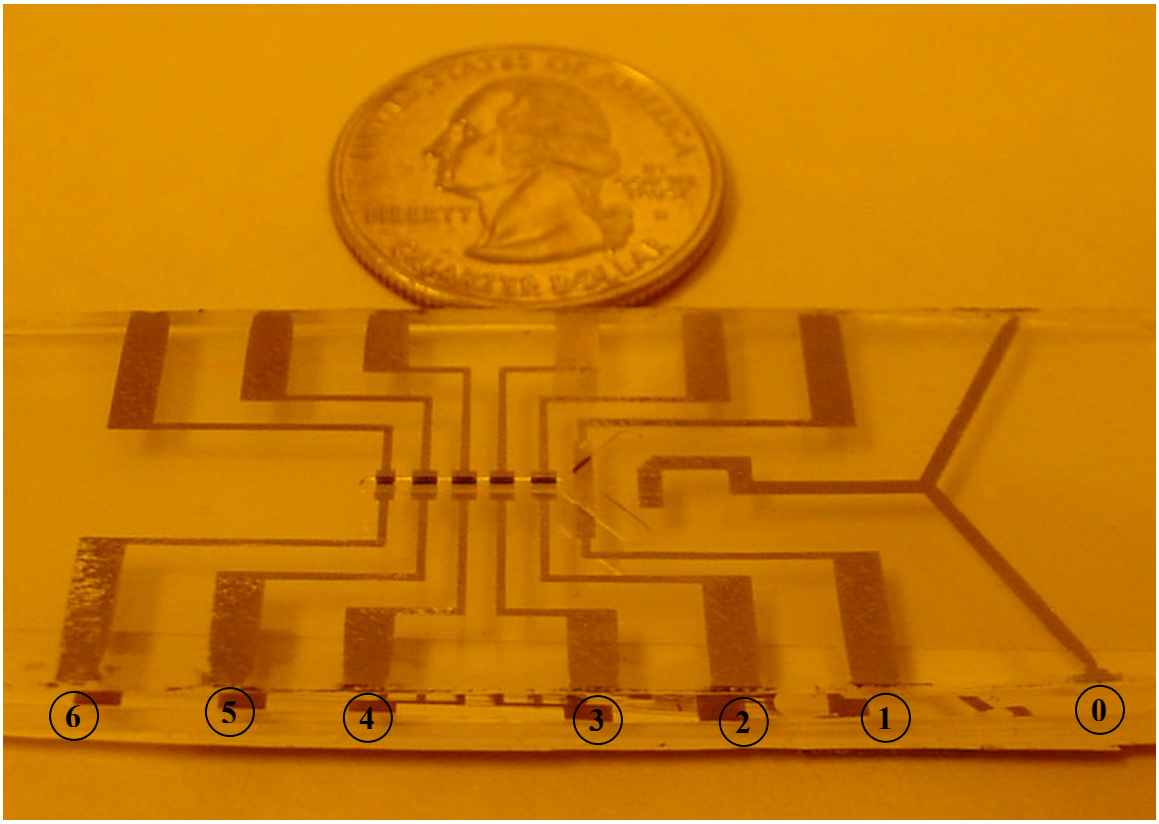

(a)

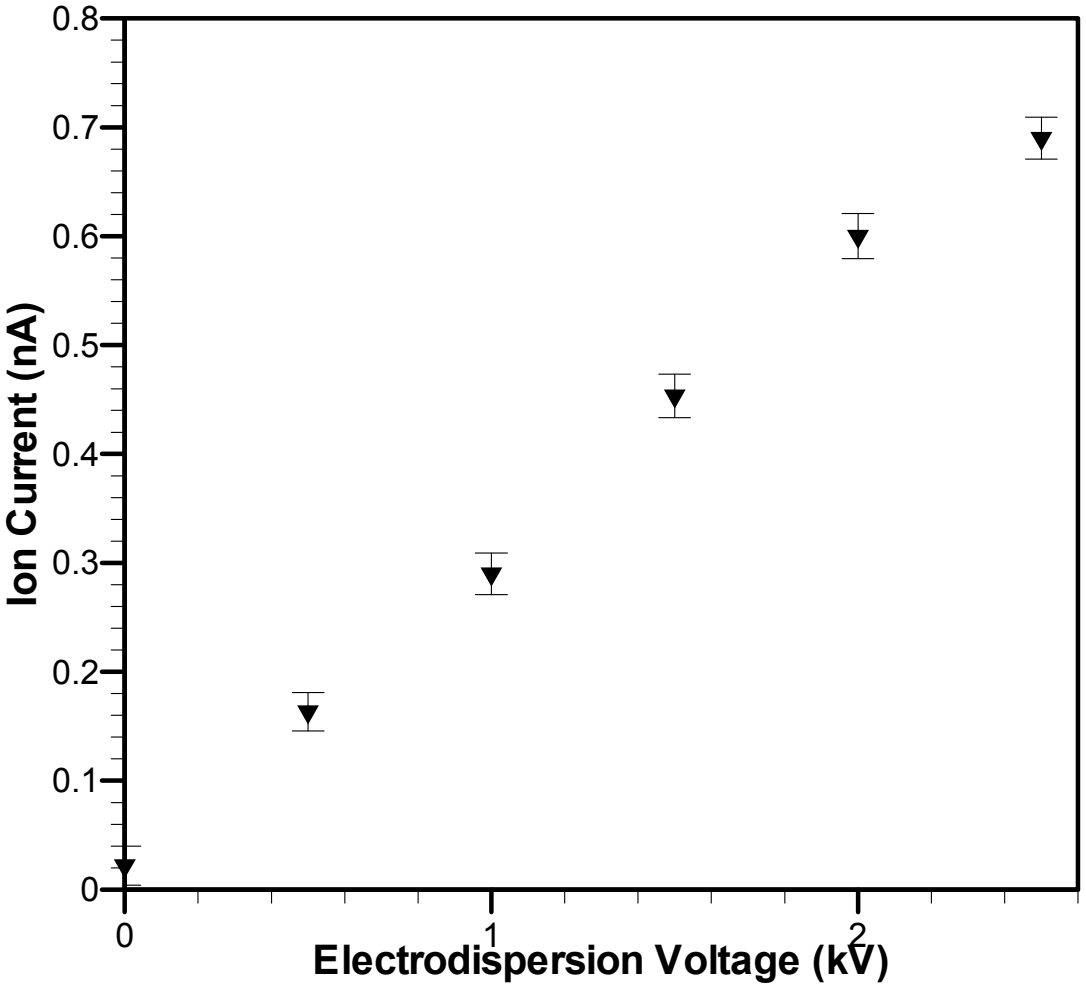

(b)

Fig. 3.5 (a) Photograph of the patterned platinum electrodes formed around and outside of the PDMS based microchannel. Electrode # 0 is connected to a high voltage power supply to ionize the sample. Electrodes # 1 to # 5 are connected to another high voltage power supply to maintain a uniform electric field along the channel, while electrode # 6 is hooked up with a current amplifier (b) Current detected by the pt- sensor to demonstrate the connectivity. Benzene and methyl alcohol (CH_3OH) - water (90:10) solution were used as the drift liquid and sample respectively for this experiment. The sample was ionized and the ions were detected by the sensor. If there was any crack or discontinuity in the electrode, sample might not be ionized and ions might not be drifted and detected.

3.5 Discussion

We developed a novel platinum electrode fabrication technique in the PDMS based microfluidic channel. This patterning technique around the PDMS microchannel would be of great use for medical analysis, environmental monitoring, biochemical analysis. Our electrode fabrication technique consists of lithography, thermal processing, sequential electrode sputtering and stripping off photoresist, while soft-lithography is used to form the microfluidic channels. In this study, the microchannel thickness was varied from 10 microns to 400 microns, while the platinum electrode thickness was kept below 350 nm to reduce the flow disturbances in the microfluidic chip. The surface roughness of platinum electrodes was between -50 nm and +50 nm, even for deep microchannels. The electrode patterning process presented in this study is very effective in obtaining a smooth and flat electrode surface with almost vertical sides. This microfabrication of platinum electrodes on PDMS offers a number of advantages. First, this process does not require any hazardous chemicals. Second, it can be used for both shallow and deep microchannel. Third, the bonding between the Ti/Pt electrode and PDMS is strong enough to withstand high pressure required for microfluidic operations. Finally, no platinum residue was observed in places where platinum was taken off.

CHAPTER FOUR

SAMPLE IONIZATION AND DETECTION OF IONS IN INTEGRATED POLYMER BASED MICORCHIP

4.1 Introduction

Ionization is the first step of ion mobility spectrometry. It was essential since 1950 when researchers concentrated on analyzing biomolecules having high molecular weight [Russel, 1994]. Especially in the late 1960's development of ionization method became inevitable for the analysis of heavier molecules in pharmaceutical and polymer industries [Smith, 2004]. As per the high demand of breaking down the molecules into ions, different ionization techniques have been developed depending on the nature of the sample and the purpose of the analysis. Some of them are [Kaewsuya, 2003]:

a. Electrospray Ionization (ESI)
b. Chemical Ionization (CI)
c. Electron Impact (EI)
d. Field Desorption/ Field Ionization (FD/FI)
e. Fast Atom Bombardment (FAB)
f. Atmospheric Pressure Chemical Ionization (APCI)
g. Thermospray Ionization (TSP)
h. Matrix Assisted Laser Desorption Ionization (MALDI)

Electrospray ionization (ESI), invented by Dr. John Bennett Fenn (USA) in the 1980s and recognized by the 2002 Nobel Prize in Chemistry, triggered a huge leap in the field of mass spectrometry (MS) as it was then possible to produce molecular ions of very large (~108 daltons) molecules [Lemière, 2001]. This ionization technique is now extensively

used to ionize synthetic polymers, pharmaceuticals, natural products, proteins, carbohydrates, DNA, and even inorganic and organometallic compounds [Smith, 2004].

4.2 Electrodispersion Ionization in the Fabricated Microchip

A polymer based nozzle was fabricated for the electrodispersion ionization. In electrodispersion ionization a liquid is fed into the nozzle having a charged surface. An electrode was sputtered in the channel to fabricate the charged surface in it. The liquid fed into the nozzle contains the substance (the analyte) that needs to be ionized. The analyte is dissolved in a large amount of solvent such as buffers, volatile acids, or bases. Due to very high voltage (kV range) the liquid molecules become heavily charged and like charges repel each other. The liquid then pushes itself out of the nozzle and forms a mist or an aerosol of small (μm sized) droplets. Towards the tip of the nozzle the charged analyte molecules are forced closer together. The proximity of the molecules becomes unstable as the similarly charged molecules come closer together. The droplets then once again explode due to the extreme Coulombic repulsion. Ions then come out of the nozzle and are carried toward the detector by the applied electric field along the channel.

4.3 Experimental

Fig. 4.1 provides a schematic representation of the microchip for electrodispersion ionization and ion detection. Detailed descriptions of the chip, along with experimental procedure, are given below

The microchip consists of a Y-shaped channel and a nozzle as shown in Fig. 4.1. Both the channel and the nozzle were fabricated on PDMS. The channel is 200-μm-deep,

1 mm wide and 10 mm long, whereas the depth of the nozzle is 12 μm. Nozzle sprays the sample ions to the drift channel and forms the Taylor cone.

There are four inlet- and exit- openings in the channel and the nozzle. Openings at the branches of the Y-channel are connected with capillaries of 280-μm-inner diameter (i. d.) and 610-μm-outer diameter. The other ends of the capillaries are open to the atmosphere. Openings at the nozzle and the end of the Y-channel are for inlet of the sample and the drift liquid respectively. On the other hand two openings at the branches of the Y-channel work as the exit ports of the drift liquid along with molecules and ions (attached to the channel walls) formed from the sample ionization. A dual-position syringe pump (Cole Parmer 74900 series, Cole Parmer Instrument Company, Illinois) pumps the sample through the capillary into the nozzle of the microchip. Drift liquid is fed into the channel from the other side in the same manner but in this case a single position syringe pump is used (11 Plus, Harvard Apparatus Inc., Massachusetts). The syringe pump provides pulseless flow at low flow rates (0.1-10 μL/min). The syringe (3 mL) used as the injector is connected to the capillary of i. d. 280 μm which performs as a transfer line of the sample. Similar configuration is also used for feeding the drift liquid in the channel. Other ends of both the capillaries are connected to the nozzle opening and the channel opening at the end.

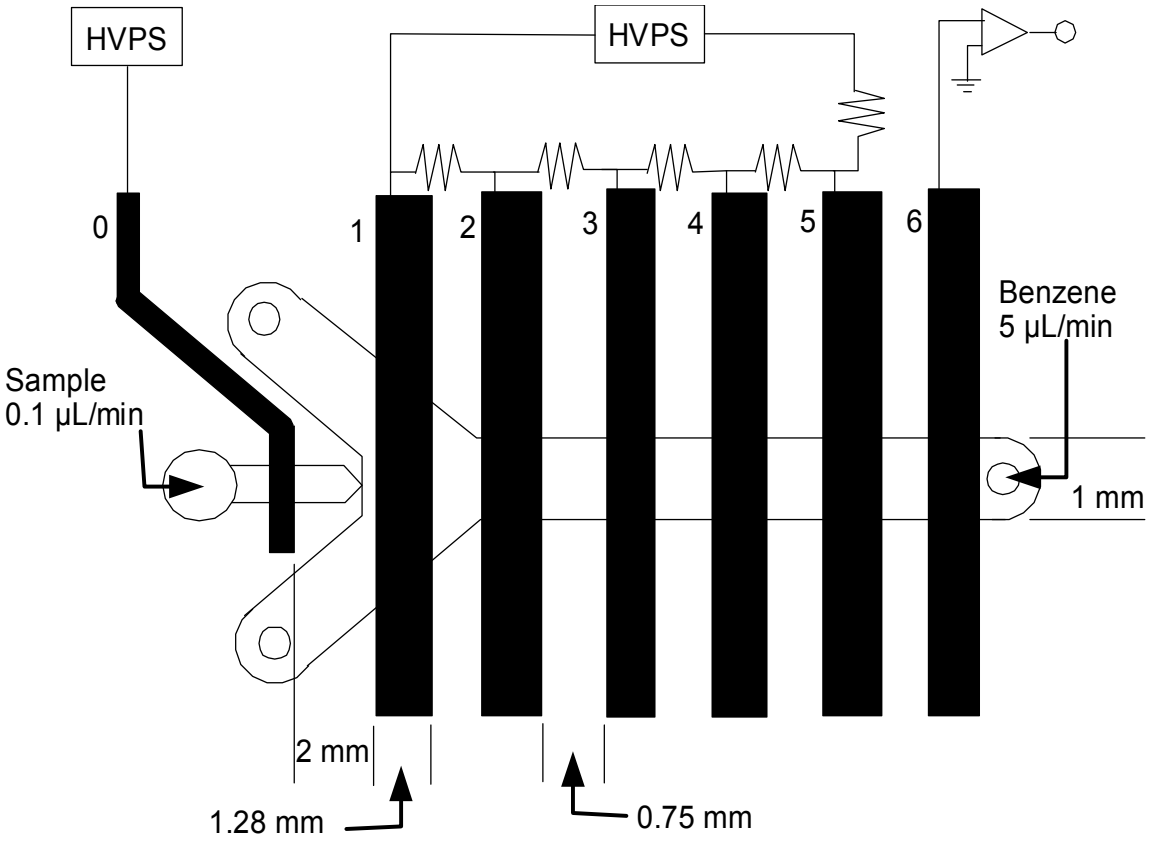

Fig. 4.1 Schematic of the microchip for electrodispersion ionization and ion detection. The microchip consists of an Y-shaped channel and a nozzle fabricated on PDMS. The channel is 200-µm-deep and the nozzle is 12-µm-deep. There are four inlet- and exit-openings in the channel and the nozzle. Openings at the nozzle and the end of the Y-channel are for inlet of the sample and the drift liquid respectively. Two openings at branches of the Y-channel work as the exit ports of the drift liquid along with molecules formed from the sample after ionization. Electrodes # 0 to # 6 are made of platinum with ~ 320 nm thick and serve for ionization of the sample, drift of ions along the channel, and detection of ions.

Six platinum electrodes of 0.75 mm apart are fabricated in the channel. The depth and width of each electrode are approximately 320 nm and 1.28 mm respectively. The first five electrodes (# 1 to # 5) from the nozzle side are used to apply the electric field and the sixth one (# 6) close to the drift liquid inlet works as the ion current detector. The purpose of applying the electric field is to drift the ions towards the detector. To have uniform electric field along the channel, the number of electrodes should be as many as possible, the width of each electrode should be as low as possible, and at the same the time electrodes should be as close as possible. There is another electrode which is fabricated in the nozzle. Its purpose is to apply very high voltage to ionize the sample. The distance between the ionization electrode and its next electrode (electrode # 1 used to apply the electric field along the channel) is 2 mm. Electrode # 1 is positioned in the channel right next to the tip of the nozzle. Otherwise the ions getting into the drift channel might be adsorbed by the PDMS surface.

The ionization electrode is connected to the high voltage power supply. Electrodes # 1 to # 5 are connected to another high voltage power supply through 2.5 MΩ (with 1% tolerance) resistors in series. The reason to use these high ohmic resistors is to avoid the damage of the resistors while high electric field is applied. The voltage rating of these resistors is 2.5 kV. The 6^{th} electrode, used as the ion current detector, is connected to a multi-meter through a current amplifier. The ion current is evaluated by dividing the voltage (in mV) obtained from the multi-meter by the current amplifier gain (in volt/ amp).

4.4 Results

The objective of this investigation is to show the ability of the developed microchip to ionize the sample and detect the ion current. This will be an initial step for

constructing a stable ionization source for the proposed polymer based miniaturized liquid phase ion mobility spectrometer.

Initial experiments served to standardize the miniaturized ion detection system at operating conditions. This was performed without sample and drift liquid in the channel. When there was no electrodispersion ionization potential, the current detected by the multi-meter was around 0.02 nA. This very low level current was probably due to noises generated from electrical instruments. Table 4.1 shows the current values at different electrodispersion potentials. Data set represents an electric field of 50 V/mm to drift ions toward the detector. With increase in ionization voltage the current values did not vary significantly from that of no voltage condition. This means that PDMS behaved as an insulator between the electrodes up to the maximum voltage applied in this investigation and provided uniform electric field along the channel.

Table 4.1 Standardization of ion detection system with electrodispersion ionization potential and electric field in the empty channel*

Ionization Voltage (kV)	**Drift Field (V/mm)**	**Measured current (nA) (Average)**
0.0	50	0.018
0.5	50	0.02
1.0	50	0.016
1.5	50	0.02
2.0	50	0.016
2.5	50	0.02

* With increase in ionization and drift voltages the current values did not vary significantly from that of no voltage condition in the empty channel.

Ion current from ionized benzene was monitored and recorded as a function of ionization potential. Fig. 4.2 shows the ionization of non-polar benzene to compare the results with that of a polar sample, mixture of Methyl Alcohol (CH_3OH) and water at a ratio of 90:10. In the first experiment, benzene was fed into the nozzle at a flow rate of 0.1 μL/min. Benzene from this side was tried to ionize by applying high voltage. From the other end of the channel benzene was also fed to sweep off molecules and ions out of the channel. The flow rate of benzene at this end was 5 μL/min, which was sufficient enough to remove the molecules and ions from the channel. Besides, applying higher flow rate might cause the dissociation of two layers of the PDMS based microchip. Without the electrodispersion ionization potential there was no current at all except the electrical noises. An ionization voltage of 0.5 kV was then applied to ionize benzene. Increase in electrodispersion voltage with a step size of 0.5 kV did not show a significant variation of ion current. This means that benzene was not ionized.

Fig. 4.2 also shows the ion current from the ionized mixture of Methyl Alcohol (CH_3OH) and water (90:10), known as sample, as a function of electrodispersion potential. Sample was fed into the nozzle at a flow rate of 0.1 μL/min and benzene was fed at the other end of the channel at a rate of 5 μL/min. Increase of the electrodispersion potential to 0.5 kV caused the ionization of the sample and an ion current of 0.16 nA was detected. With increase in the electrodispersion voltage, more ion current was detected. The drift field was maintained 50 V/mm along the channel during the experiment. It is expected that there should be a threshold ionization potential beyond which the ion

current should be constant which is probably higher than 2.5 kV. But due to the limitation of the high voltage power supply it was not possible to increase the voltage above 2.5 kV.

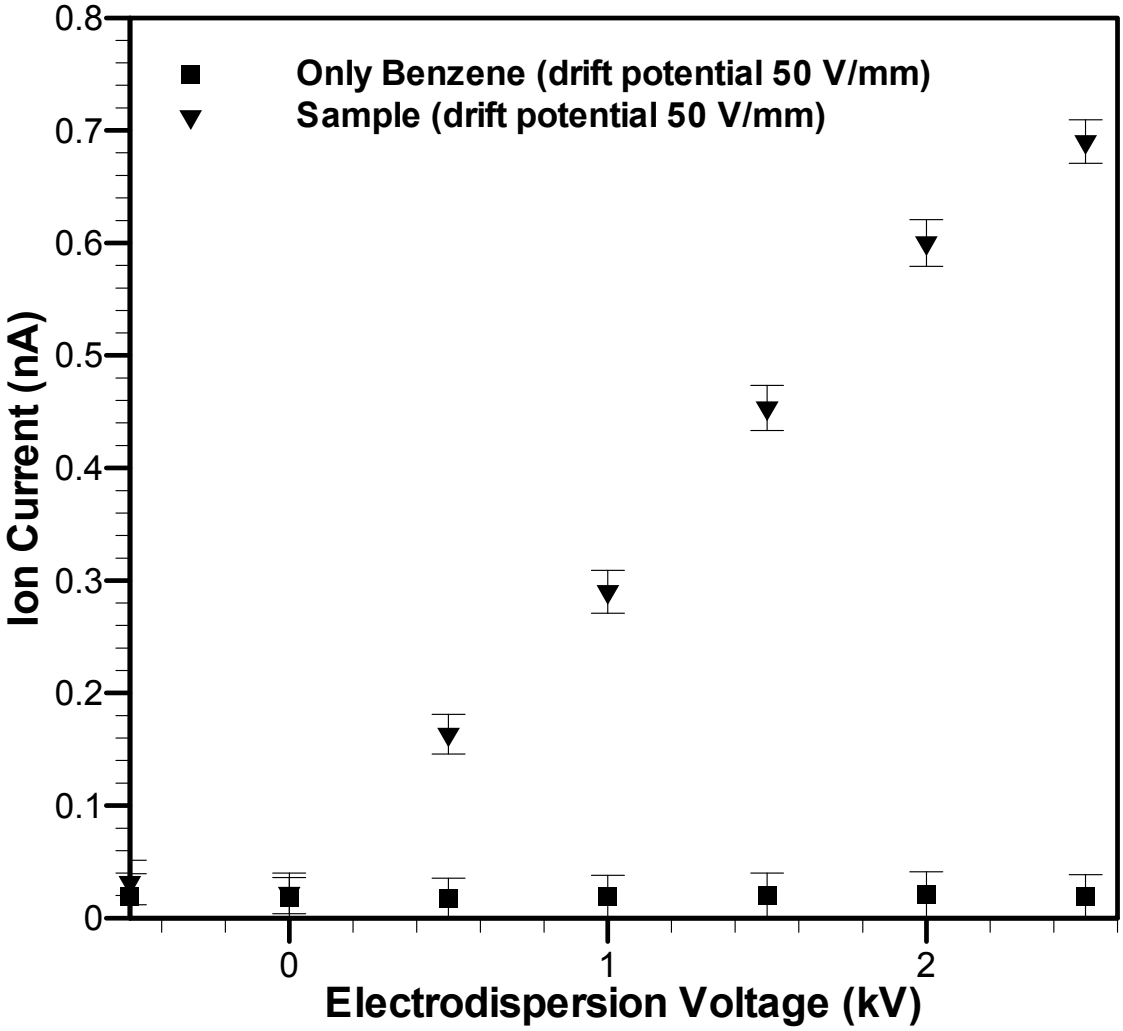

Fig. 4.2 Ionization of Benzene and 90: 10 Methanol: Water (sample) in the polymer based microchip. First benzene was fed into the nozzle and at the end of the drift channel at flow rates of 0.1 μL/min and 5 μL/min respectively. However no significant current was detected at different electrodispersion ionization (EDI) potentials meaning that benzene was not ionized. The drift field was 50 V/mm. When the sample was fed into the nozzle at the same flow condition and at the same drift field, significant current was observed at different EDI potentials.

4.5 Discussion

In order to focus ions into the center of the drift region where the electric field was uniform, the nozzle was aligned to the centerline of the drift channel. This reduced the loss of ions at the channel walls. Ionizations of both polar and non-polar samples were tested and good electrodispersion ionization for polymer based ion mobility spectrometer was achieved from the above experiments. So it can be concluded that the newly developed miniaturized microchip is capable enough to generate sufficient ions for ion mobility spectrometer.

CHAPTER FIVE

RESULTS AND DISCUSSION

5.1 Microchip for Ion Detection

In this study we developed a polymeric microchip for ionization and detection of ions in liquid phase as shown in Fig. 5.1. The crucial part of this work is to integrate the ionization source with the drift system because it is extremely essential for the miniaturization of such devices in field applications. This also simplifies the components required to build and assemble the IMS setup. As mentioned in chapter 2, we fabricated a nozzle and placed it at the entrance of the drift channel along its center line.

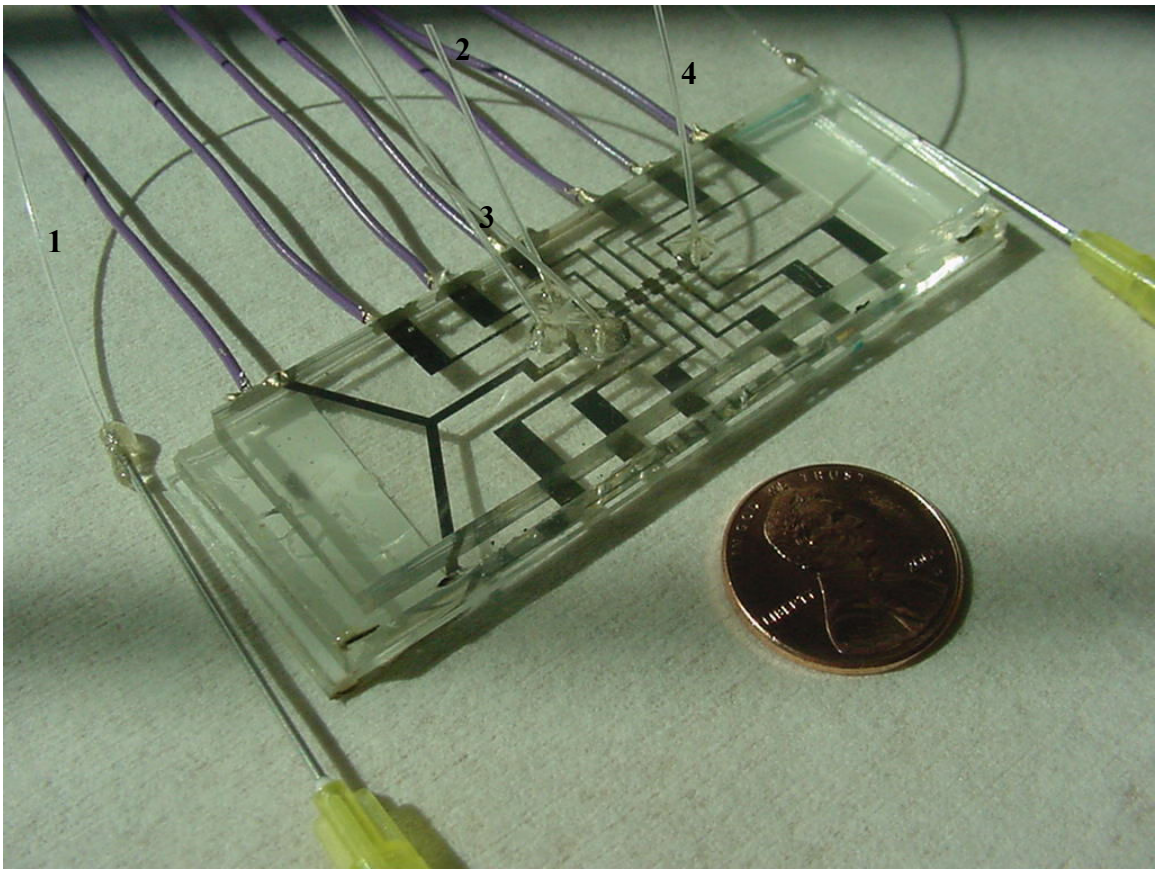

Fig. 5.1 Photograph of the ion detection microchip for liquid phase ion mobility spectrometry.

Four capillaries (# 1 - # 4) are shown in this picture. Capillary # 1 feeds the sample into the nozzle and capillary # 4 feeds the drift liquid into the drift channel. Capillaries # 2 and # 3 take the drift liquid along with unwanted molecules out of the chip. There are seven platinum electrodes each of ~ 320-nm-deep are sputtered which are also shown in Fig. 5.1. One of them is used for ionizing the sample (the left most one in the picture); next five electrodes are for drifting the ions to the last electrode which serves as an ion current detector. To connect electrodes to the high voltage power supply wires are connected with them by silver epoxy (shown in Fig. 5.1). Then the chip is ready for ionization of the sample and detection of the ion current.

5.2 Voltage Verification

To detect ions after ionization, they are drifted along the channel towards the detector. It is possible by applying a drift voltage along the channel. The electrodes were connected with each other in series by 2.5 MΩ resistors. Five resistors were required to connect the electrodes with high voltage power supply. A multimeter measured the drop of voltages along the channel when the channel was filled with the drift liquid (benzene) at a flow rate of 5 μL/min. The voltage verification was performed by applying 500 V, 1000 V, 1500 V, and 2000 V. It was found that the potential drop across each resistor along the channel was almost constant in each case as expected (as shown in Table 5.1). However there was a difference between the expected potential drop across each resistor and the measured value. For example, when 500 V was applied across five resistors, an average potential drop of about 83 V was measured by the multimeter. But the expected average potential drop across each resistor should be 100 V (500 V/ 5 = 100 V). So a difference of 17 V was observed. Similarly, for a drift potential of 1000 V it is expected that 200 V should be dropped across each resistor. However a potential drop of an average of 166 V was observed. For a drift potential of 1500 V, the average measured

potential drop was 248 V and for 2000 V drift potential, approximately 332 V potential drop was measured.

Table 5.1 Potential drop across each resistor at different drift voltages.

Drift voltage (V)	Potential drop (in Volt) at				
	Resistor # 1	Resistor # 2	Resistor # 3	Resistor # 4	Resistor # 5
500	83.04	83.0	83.85	82.87	82.7
1000	165.6	166.16	167.84	165.51	166.25
1500	248.37	249.13	249.43	250.78	248.67
2000	331.71	332.34	333.05	331.84	332.05

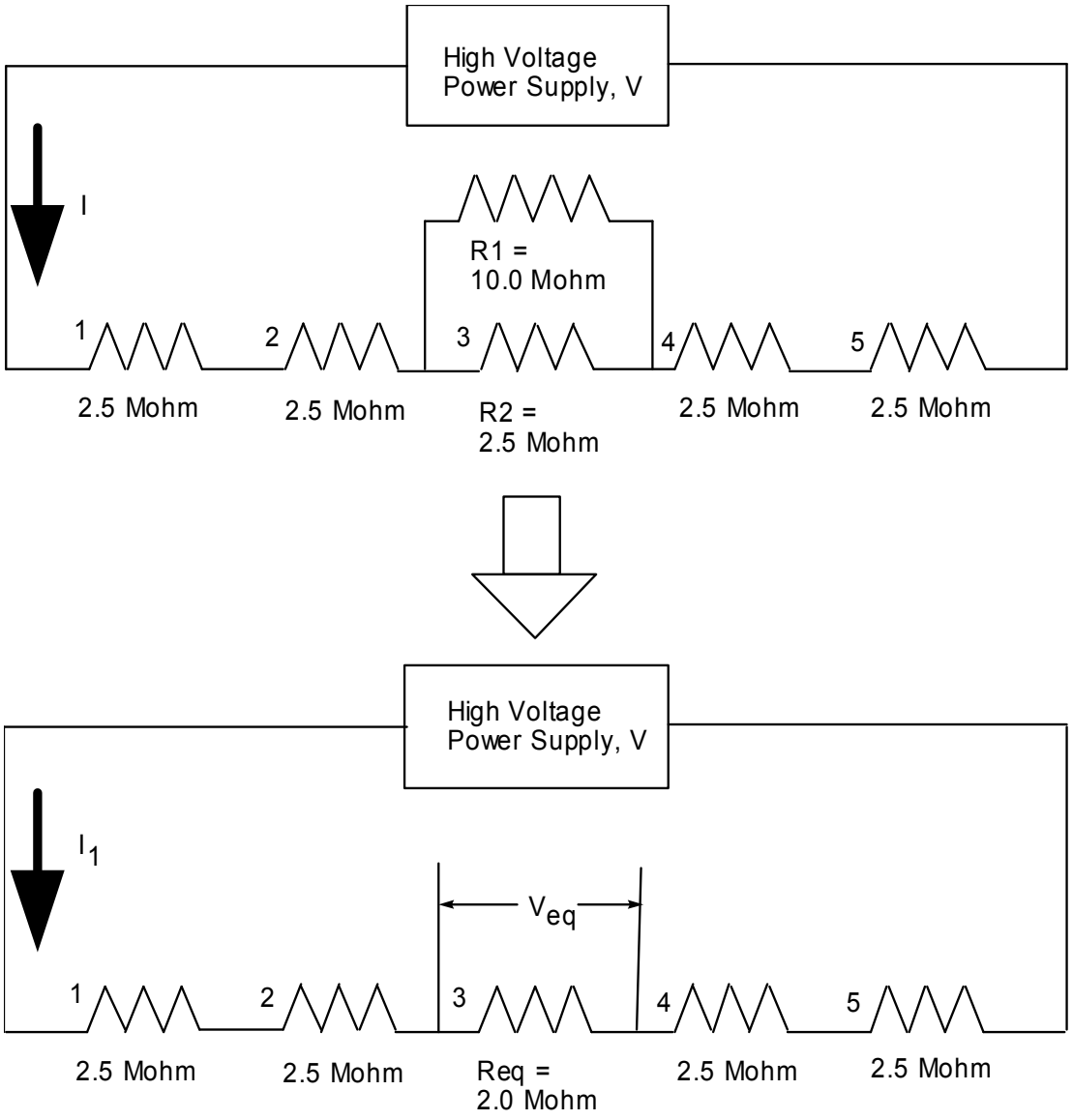

Fig. 5.2 Circuit diagram for the calculation of voltage drop across each resistor in the drift system.

Fig.5.2 shows the circuit diagram for applying the drift potential along the channel and measuring the potential drop across each resistor. The multimeter used to measure the potential drop has a resistance of 10 MΩ. When it was connected to the circuit this resistance became a parallel resistance with 2.5 MΩ resistor in the circuit. As the multimeter resistance and the circuit resistance were the same order of magnitude,

hence the multimeter resistance affected the drift voltage circuit. Let us consider the following calculation:

Multimeter resistance, $R_1 = 10.0\ M\Omega$

Each circuit resistor, $R_2 = 2.5\ M\Omega$

Equivalent resistance, $R_{eq} = \frac{R_1 . R_2}{R_1 + R_2}$

$$= \frac{10.0 \text{ x } 2.5}{10.0 + 2.5}$$

$$= 2.0\,M\Omega$$

Total resistance in the equivalent circuit, $R_{tot.,\,eq} = 2.5\ M\Omega \text{ x } 4 + 2.0\ M\Omega = 12.0\ M\Omega$

If a voltage of 500 V is applied as the drift voltage, then

Current in the circuit, $I_1 = \frac{V}{R_{tot.,eq}} = \frac{500\,V}{12.0 \text{ x } 10^6\ \Omega} = 41.67\,\mu A\,(app.)$

So the potential drop across the equivalent resistor, $V_{eq} = I_1\ R_{eq}$

$$= (41.67\ \mu A)\ (2.0\ M\Omega)$$

$$= 83.34\ V$$

Hence the calculated potential drop while measured with the multimeter is almost equal to that of the measured value. A slight deviation is due to the tolerance of the resistors. According to the manufacturer, the resistors have 1% tolerance.

Actual resistance values and corresponding potential drops across each resistor for the 500 V drift potential have been calculated in Appendix. Average voltages at different

electrodes have been plotted in Fig. 5.3. It shows that the potential drops are linear and smooth in all cases of drift potentials, as they should be.

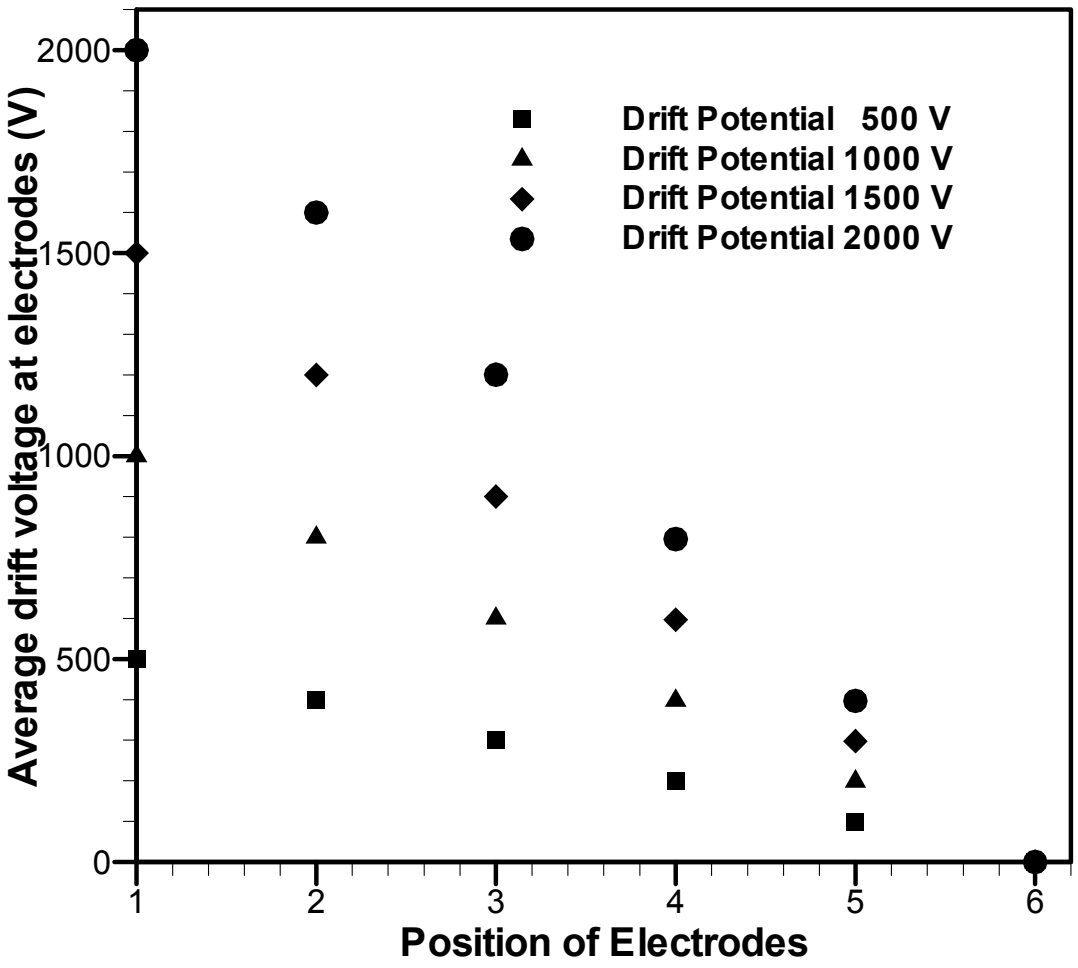

Fig. 5.3 Average drift potentials at different electrodes. Benzene flow rate was maintained 5 μL/min during the experiment. The plot shows linear potential drop along the channel in all cases. Positions 1 to 5 refer to electrodes and position 6 refers to the ground end of the high voltage power supply.

5.3 Electrodispersion Voltage Characterizations

The relationship between the total ion current and the applied electrodispersion voltage was observed for the device at a flow rate of 0.1 μL/min of sample 90:10 methyl alcohol : water. The sample was pumped through the nozzle to the drift channel and the non- polar liquid, benzene, was pumped at a flow rate of 5 μL/min from the other end of the channel. The voltage difference between # 0 and # 1 refers to the electrodispersion voltage (as shown in fig. 4.1). For example if a voltage of 1000 V is applied at electrode # 0 and 500 V between electrode # 1 and # 5, then the difference of 500 V will be the electrodispersion ionization voltage. In this experiment the electrodispersion voltage was increased at a step size of 0.5 kV up to 2.5 kV when the drift voltage was 500 V, and up to 2.0 kV when the drift voltage was 1000 V. The total ion current each voltage was plotted against the applied electrodispersion voltage as in Fig. 5.4 (a, b).

For electrodispersion ionization, a very high electric field in the nozzle electrically charges the sample liquid. This generates the plume of droplets of liquid. The charged liquid in the nozzle becomes unstable as it is forced to hold more and more charge and search for a potential surface of opposite charge so that they are able to de-energized. Due to their motion in the nozzle, the solvent molecules evaporates from their surfaces and causes the charged droplets shrink down. Since it is difficult for charges to evaporate, the charge density in the droplets becomes dramatically increased.

The charged liquid while pushed toward the tip of the nozzle, it is then forced to hold more and more charges. As the droplets do not find an oppositely charged surface in which it could dissipate its charge in time, the electrical charge reaches a critical state and the droplet violently blows apart and forms the cloud of ions at the tip of the nozzle [Newobjective's website]. This was first observed by the renowned physicist John Zeleny in 1914 [Zeleny, 1914].

In Fig. 5.4, as the electrodispersion voltage was increased the total ion current also increased. This is obvious as increase in electrodispersion voltage causes more sample to ionize. However, after a certain voltage the ion current should remain constant. Because at that threshold voltage all the sample molecules become ionized and are detected by the detector. The trend of increase of ion current with increase in electrodispersion ionization voltage was also observed for the drift voltage of 1000 V.

However, a little more ion current was observed at the same electrodispersion voltage but higher drift potential. In Fig. 5.4, applying a drift voltage of 1000 V (100 V/mm) caused more ion current than that of at 500 V (50 V/mm). This is because the loss of some ions at the channel surface was probably avoided at a higher drift field.

This was investigated in both negative and positive mode. In the negative mode, when both the electrodispersion voltage and the drift voltage were negative, negative ions could only pass through the drift channel, whereas, positive ions dissipated their energy at the oppositely charged surface and could not reach the detector. In this experiment, the possible negative ions were OH^- (hydroxyl-) ions. In case of positive mode, when the electrodispersion voltage and the drift voltage were positive, positively charged ions could reach the detector only.

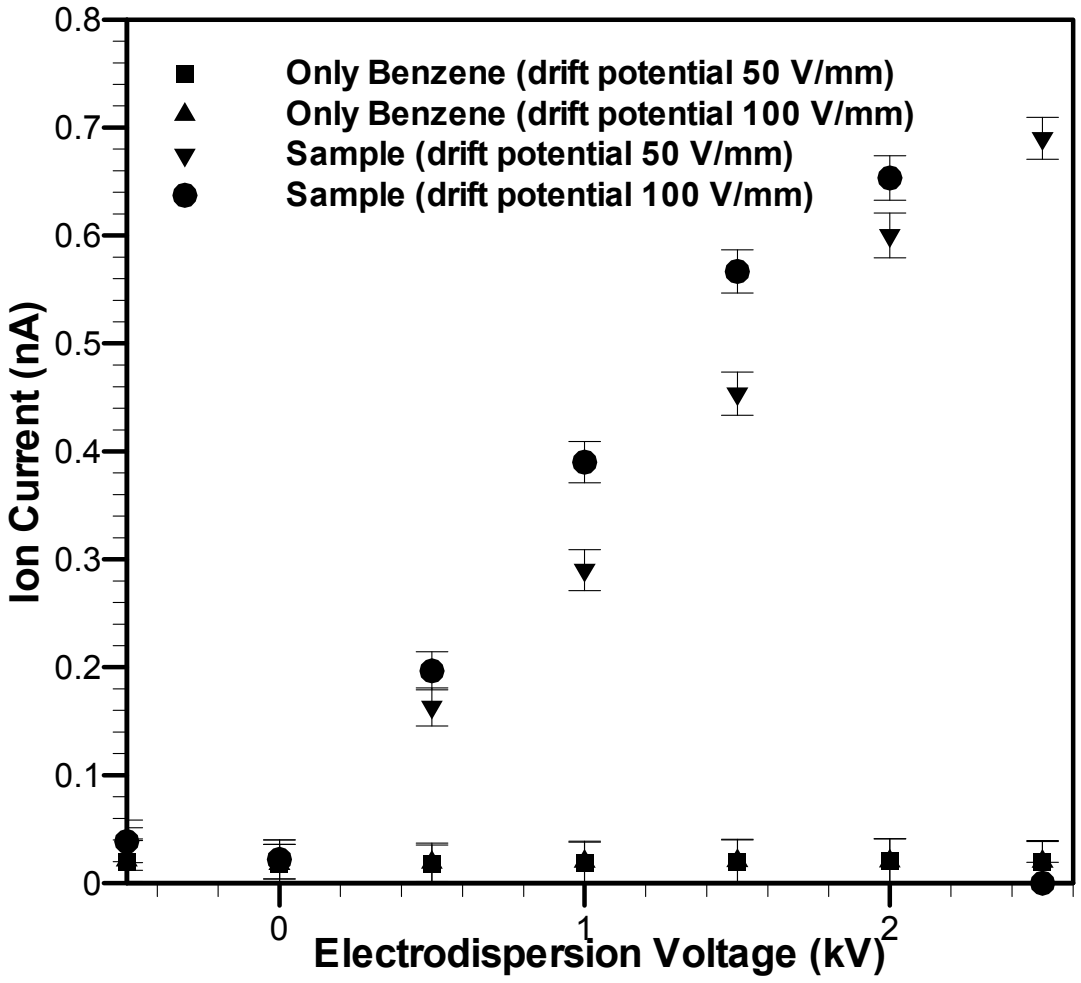

Fig. 5.4 (a) Relationship between ion current and electrospray voltage. The sample 90:10 methyl alcohol : water was pumped into the nozzle at a flow rate of 0.1 μL/min. The benzene flowed in the opposite direction at a rate of 5 μL/min. The drift voltages were 500 V and 1000 V. Benzene was also tried to ionize, but there was no significant current observed. This experiment was carried out in (-) ve mode.

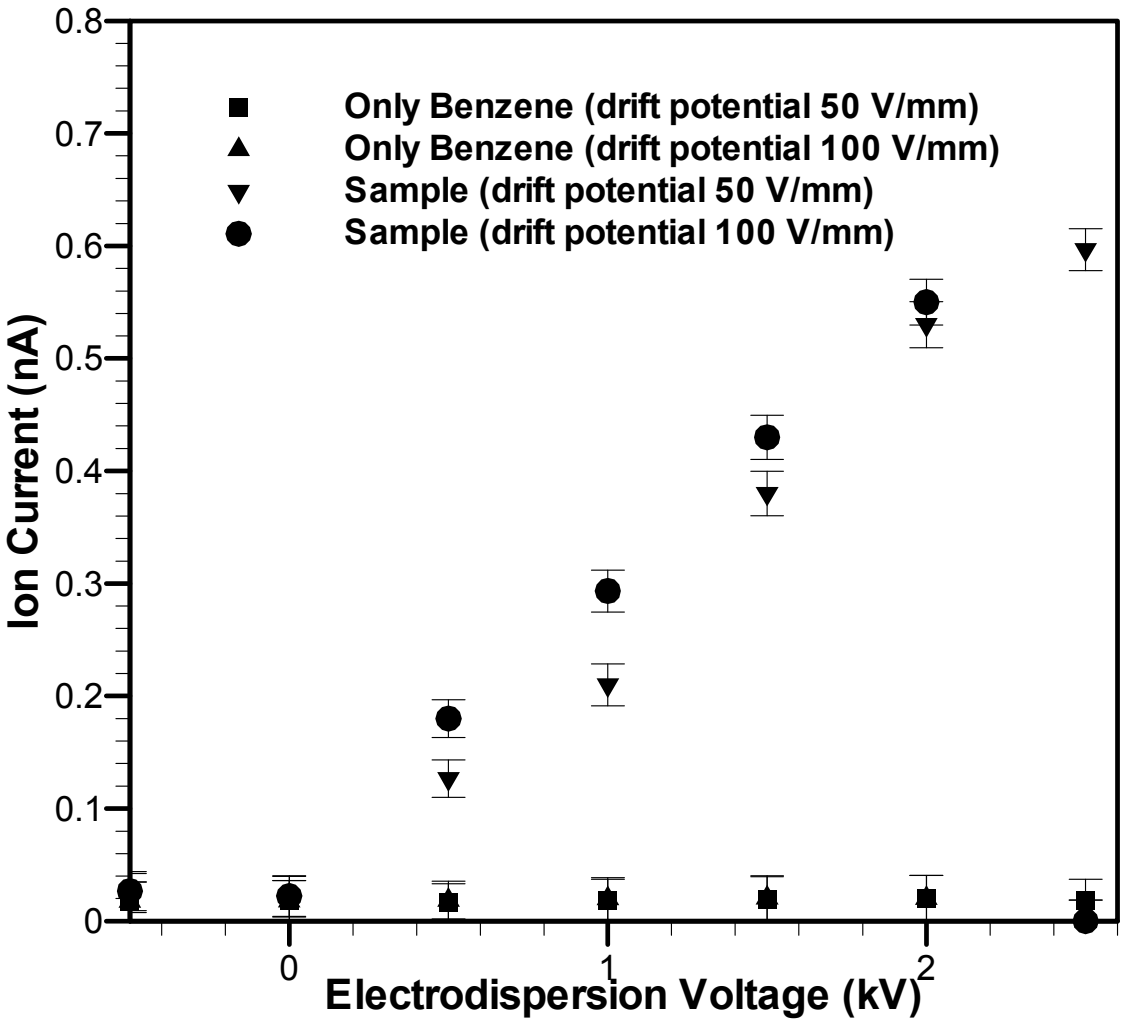

Fig. 5.4 (b) Relationship between ion current and electrospray voltage. The sample 90:10 methyl alcohol : water was pumped into the nozzle at a flow rate of 0.1 μL/min. The benzene flow rate was maintained 5 μL/min. The drift voltages were 500 V and 1000 V. This experiment was carried out in (+) ve mode. The noise level of the current was around 0.016 nA.

5.4 Uncertainty

There are several sources of uncertainties both in fabrication and in the experiment. Table 5.1 shows a list of sources that causes uncertainties in current measurement and in widths and depths of the nozzle and the drift channel.

Table 5.2 Sources of uncertainty in fabrication and current measurement.

Input Parameter	**Relative Uncertainty (Absolute or %)**
Spin Coat	± 4% *
Baking	± 5.26% *
Intensity of Photolithography lamp	± 2% †
Alignment	± 8.75% *
Resistors	± 1% *
Multimeter	± 0.1% †
Syringe Pump	± 5.5% ‡
Current Amplifier	± 2% **

* Experimental

† Manufacturer

‡ Salgado et al., 2006

** http://www.testequipmentconnection.com/Test-Equipment-Detail.asp?model=427

Resistivity is a function of temperature. There is a possibility of heat generation as well as temperature rise at electrodes due to high voltages used in this experiment. It was

not possible to measure that temperature. However taking this into an account there would be an effect on ion current measurement due to the elevated temperature.

Another possible source of uncertainty is the preparation of the sample. A solution of 90:10 methanol : water was prepared for ionization. There is a possibility of human error in this preparation.

Two high voltage power supplies and a current amplifier were used in this experiment. Unwanted noise generated during the operation of power supplies and other electrical and electronic equipment might cause a deviation between actual and displayed potential drops.

5.5 Safety Considerations

It was mentioned above that high voltages were required in the experiments. Hence proper insulation and necessary shielding were used along with regular safety measures. This was to ensure that the high voltage power supply is sufficiently current limited so as not to be fatal in case of accidental contact.

In this experiment benzene was used as the drift liquid due to its non polar characteristics and potential stability at high voltages. However, it is dangerous, toxic, flammable and carcinogenic. “It is considered harmful by ingestion, inhalation, and dermal exposure routes. It is also irritating to the eyes and skin. Excessive inhalation results in heartbeat irregularities and adverse central nervous system effects including headache, sleepiness, dizziness, nausea, loss of coordination, tremors, and in extreme conditions, coma and death. Systemic absorption effects may include long-term damage to the blood-forming system, kidney and liver damage, and/or cancer (leukemia).

Ingestion may also cause adverse effects on central nervous system, blood disorders, kidney and/or liver damage [Novachem's website]."

Methyl alcohol is irritant to skin and eye and hazardous in case of ingestion and inhalation [Sciencelab's website]. As potentially toxic or flammable materials were used or sprayed in this study, proper ventilation and vapor removal were provided. The experiment was conducted under the flume hood with proper ventilation and vapor removal facilities. Moreover precautions and safety practices were followed for proper handling of all the chemicals used in the experiment.

CHAPTER SIX

CONCLUSION

6.1 General

This research is comprised of two major aspects. The first part is the design and fabrication of a polymeric microchip to ionize and detect ions of different chemical samples for liquid phase ion mobility spectrometry. The second part is the demonstration of this microchip's workability. This chapter includes the major conclusions that can be made from the entire work, limitations, and future improvements of this research.

6.2 Achievements

This is the first time a polymeric based microchip for chemical sample ionization and detection of ions has been developed. Poly-di-methyl-siloxane (PDMS) was used to fabricate the microchip. It is highly transparent, behaves as an insulting material, and is chemically inert. These properties make it indispensable for this microfluidic device essentially to detect the hazardous biomolecules and explosives. A nozzle has been introduced in the system for ionization, which eliminates an externally placed capillary at the entrance of the drift channel.

A novel platinum-electrode fabrication technique in the PDMS based microfluidic channel has been developed. This electrode fabrication technique consists of lithography, thermal processing, sequential electrode sputtering and stripping off photoresist. SU-8 (2010) was used to pattern the electrodes in the channel. It is observed that the bonding strength between PDMS and SU-8 is very poor, because PDMS has extremely low surface energy (19.8 mJ/m^2). Utilizing this favorable surface property SU-8 was stripped-off from the PDMS surface leaving behind the patterned electrodes in the channel.

Besides, sputtered metals and additional hard bake increased the brittleness of SU-8 and facilitated easy removal of metal-coated photoresist from the PDMS surface.

This microfabrication of platinum electrodes on PDMS offers a number of advantages:

i. this process does not require any hazardous chemicals;
ii. it can be used for both shallow and deep microchannel;
iii. the bonding between the Ti/Pt electrode and PDMS was found strong enough to withstand high pressure required for microfluidic operations;
iv. no platinum residue was observed in places where platinum was taken off.
v. it was observed in this study that the surfaces of electrodes were quite smooth and flat with almost vertical sides.

Finally without this fabrication technique it would not be possible to develop polymeric microchips with embedded Pt-electrodes for medical analysis, environmental monitoring, biochemical analysis where even gold electrodes are reactive to many biomolecules.

Ionization was demonstrated by ionizing benzene and 90: 10 Methanol: water. Then the ion currents were compared between these two cases. As benzene is a non-polar liquid, it won't be ionized as compared to other polar samples. It is found in this study that benzene was not basically ionized; however, significant ion current was detected from the ionization of methanol-water solution. The ion current increased with increase in electrodispersion ionization voltage because increase in the voltage caused more ions to be generated from the sample. Another important observation is that the drift voltage has also an effect on ion current, as more ions are then carried over towards the detector. At low drift voltage, some ions get lost due to the lack of sufficient energy to move down to the channel and get stick to the PDMS surface. This study also demonstrates the

detection of both positive and negative ions. Ionization process always creates these two types of ions. Using two different voltage modes it was possible to detect these two different types of ions.

6.3 Limitations of the Present Work

This is the first study of ionization and ion detection in liquid phase in an integrated module in the microscale. For this reason no quantitative comparison of ion current is established for this work. However in gas phase macroscale ion mobility spectrometry, the ion current is almost of the same order of magnitude that obtained in this study. The power supplies used in the experiment are limited by the maximum voltage of 3.0 kV. For this reason it was not possible to reach up to the saturation level of ionization where increase in electrodispersion voltage would not increase the ion current, as possible number of ions have already generated.

6.3 Future Work

The platinum microelectrodes fabricated in the microchip are of 1.28 mm wide and 0.75 mm spaced from the adjacent one. So the potential drop along the channel is not smoothly linear rather step wise. There is an equivoltage along the width of each electrode. To avoid this, the width of electrodes needs to be reduced and the number of electrodes should be increased. No gate has yet been applied to control the ion flows. Hence to do this, an electric field will be established between one of the top layer electrodes and its opposite bottom layer electrodes. This requires some extra fabrication to make insulation between these two electrodes. Currently these two electrodes are in contact to form a ring of electrode inside the channel. The gate might also be introduced by controlling the sample flow.

BIBLIOGRAPHY

Adams, M. L.; Johnston, M. L.; Scherer A.; Quake, S. R.; "Ploydimethylsiloxane based microfluidic diode," *Journal of Micromechanics and Microengineering* **15**, 1517-1521 (2005).

Alarie J. P.; Jacobson S. C.; Ramsey J. M.; "Electrophoretic injection bias in a microchip valving scheme," *Electrophoresis* **22**, 312–317 (2001).

Anderson, R.C.; Bogdan, G.J.; Bamiv, Z.; Dawes, T.D.; Winkler, J.; Roy, K.; "Microfluidic bischemical analysis system," in *International Conference on Solid State Sensors and Actuators*, pp. 477-480 (1997).

Asbury, G. R.; Wu, C.; Siems, W. F.; Hill, H. H. Jr.; "Separation and identification of some chemical warfare degradation products using electrospray high resolution ion mobility spectrometry with mass selected detection", *Analytica Chimica Acta* **404 (2)**, 273-283 (2000).

Bacon, A. T.; Getz, R.; Reategui J.; "Ion-mobility spectrometry tackles though process monitoring," *Chem. Eng. Prog.* **87 (6)**, 61-64 (1991).

Bacon, A. T.; Reategui, J.; Getz, R.; Fafaul, E.; Smith, D.; "Development of a gas and vapor monitor based on ion mobility spectrometry", in *Proc. Instrum. Soc. Am*. 90th conf., pp. 679 (1990).

Barry, R. and Ivanov, D.; **"**Microfluidics in biotechnology," *J. Nanobiotechnology* **2 (2)**, 1-5 (2004).

Baumbach, J. I. and Eiceman, G. A.; "Ion mobility spectrometry: Arriving on site and moving beyond a low profile," *Applied Spectroscopy* **53 (9)**, 338A- 355A (1999).

Becker, H. and Locascio, L. E.; "Polymer microfluidic devices," *Talanta* **56**, 267–287 (2002).

Boone, T. D.; Fan, Z. H.; Hooper, H. H.; Ricco, A. J.; Tan, H.; Williams, S. J.; "Plastic advances microfluidic devices," *Anal. Chem.* **74(3)**, 78A-86A (2002).

Brahmasandra, S. N.; Ugaz, V. M.; Burke, D. T.; Mastrangelo, C. H.; Burns, M. A.; "Electrophoresis in microfabricated devices using photopolymerized poly(acrylamide) gels and electrode-defined sample injection," *Electrophoresis* **22(2)**, 300–311 (2001).

Brokenshire, J. L.; Dharmarajan, V.; Coyne, L. B.; Keller, J.; "Near real time monitoring of TDI vapor using ion mobility spectrometry (IMS)," *J. Cell. Plast.* **26**, 123-142 (1990).

Burns, M. A.; Johnson, B. N.; Brahmasandra, S. N.; Handique, K.; Webster, J. R.; Krishnan, M.; Sammarco, T. S.; Man, P. M.; Jones, D.; Heldsinger, D.; Mastrangelo, C. H.; Burke, D. T.; "An integrated nanoliter DNA analysis device," *Science* **282**, 484-487 (1998).

Chauhan, M.; Harnois, J.; Kovar, J.; Pilon, P.; "Trace analysis of cocaine and heroin in different customs scenarios using a custom-built ion mobility spectrometer," *J. Can. Soc. Forensic Sci.* **24(1)**, 43-49 (1991).

Chiou C. H.; Lee, G. B.; Hsu, H. T.; Chen, P. W.; Liao, P. C.; "Micro devices integrated with microchannels and electrospray nozzles using PDMS casting techniques," *Sensors and Actuators B* **86**, 280-286 (2002).

Chovan T. and A. Guttman; "Microfabricated devices in biotechnology and biochemical processing," *Trends in Biotechnology* **20 (3)**, 116-122 (2002).

Clowers B. H.; Dwivedi, P.; Steiner W. E.; Hill, H. H. Jr.; "Separation of sodiated isobaric disaccharides and trisaccharides using electrospray ionization-atmospheric pressrue ion mobility-time of flight mass spectrometry," *J Am Soc Mass Spectrom* **16**, 660-669 (2005).

Davies, J. P.; Blackwood, L. G.; Davis, S. G.; Goodrich, L. D.; Larson, R. A.; "Design and calibration of pulsed vapor generators for 2,4,6-trinitrotoluene, cyclo-1,3,5-trimethylene-2,4,6-trinitramine, and pentaerythritiol tetranitrate," *Anal. Chem.* **65 (21)**, 3004-3009 (1993).

http://www.dowcorning.com/DataFiles/090007c880003841.pdf

Eiceman, G. A.; Blyth, D. A.; Shoff, D. B.; Snyder, A. P.; "Screening of solid commercial pharmaceuticals using ion mobility spectrometry," *Anal. Chem.* **62 (14)**, 1374-1379 (1990).

Eiceman, G. A. and Karpas, Z.; Ion Mobility Spectrometry, CRC Press, 1993, 156.

Eiceman, G. A. and Karpas, Z.; Ion Mobility Spectrometry, CRC Press, 1993, 160 (and references therein).

Eiceman, G. A.; Nazarov, E. G.; Miller, R. A.; "A micro-machined ion mobility spectrometer-mass spectrometer," *IJIMS* **3**, 15-27 (2000).

Fetterolf, D. D. and Clark, T. D.; "Detection of trace explosive evidence by ion mobility spectrometry," *J. Forensic Sci.* **38(1)**, 28-39 (1993).

Fetterolf, D. D.; Donnelly, B.; Lasswell, L. D.; "Portable instrumentation: new weapons in the war against drugs and terrorism," in *SPIE Proc.* **2092**, pp. 40-52 (1994).

Figeys, D. and Pinto, D.; "Lab-on-a-chip: A revolution in biological and medical sciences," *Analytiacal Chemistry* **report**, 330A- 335A (2000).

Fu, L. M. and Yang, R. J.; "Low-voltage driven control in electrophoresis microchips by traveling electric field," *Electrophoresis* **24***,* 1253–1260 (2003).

Gottschlich, N.; Jacobson, S. C.; Culbertson, C. T.; Ramsey, J. M.; "Two-dimensional electrochromatography/capillary electrophoresis on a microchip," *Anal. Chem*. **73**, 2669-2674 (2001)

Hallowell, S. F.; Davies, J. P.; Gresham, G. L.; "Qualitative/semiquantitative chemical characterization of the Auburn Olfactometer," in *SPIE Proc.* 2276, pp. 437-448 (1994).

Harrison, D. J.; Fluri, K.; Seiler, K.; Fan, Z.; Effenhauser, C. S.; Manz A.; "Micromachining a miniaturized capillary electrophoresis-based chemical analysis system on a chip," *Science* **261**, 895-897 (1993).

Hasselbrink, E. F., Jr.; Shepodd, T. J.; Rehm, J. E.; "High-pressure microfluidic control in lab-on-a-chip devices using mobile polymer monoliths," *Analytiacal Chemistry* **74**, 4913-4918 (2002).

Helmke B. P. and Minerick A. R.; "Designing a nano-interface in a microfluidic chip to probe living cells: Challenges and perspectives," in *Proc. of the National Academy of Sciences in the United States of America (PNAS)* **103**, pp. 6419-6424 (2006)

Hill, H. H. and Tam, M., "Ion mobility spectrometry method and apparatus," Washington State University Research Foundation, USA, U.S. Pat. Appl. Publ. (2005), 19 pp., US 2005109930.

Hiratsuka, A.; Kojima, K.; Suzuki, H.; Muguruma, H.; Ikebukuro, K.; Karube, I.; "Integration of microfabricated needle-type glucose sensor devices with a novel thin-film Ag/AgCl electrode and plasma-polymerized thin film: mass production techniques," *Analyst* **126 (5)**, 658-663 (2001).

Hong, J. W.; Hosokawa, K.; Fujii, T.; Seki, M.; Endo, I.; "Microfabricated polymer chip for capillary gel electrophoresis," *Biotechnol. Prog.* **17**, 958–962 (2001).

Hur, S. H.; Khang, D. Y.; Kocabas, C.; Rogers, J. A.; "Nanotransfer printing by use of noncovalent surface forces: applications to thin-film transistors that use single-walled carbon nanotube networks and semiconducting polymers," *App. Phy. Lett.*, **85 (23)**, 5730-5732 (2004).

Jacobson, S. C.; Moore, A. W.; Ramsey, J. M.; "Fused quartz substrates for microchip electrophoresis," *Anal. Chem.* **67**, 2059-2063 (1995).

Jacobson, S. C. and Ramsey, J. M.; "Electrokinetic focusing in microfabricated channel structures," Anal. Chem. **69**, 3212-3217 (1997).

Kaewsuya, P.; "The mechanisms of electrospray ionization process," Literature Seminar, Dept. of Chemistry, The University of Alabama, 2003.

Karasek, F. W.; Kilpatrick, W. D.; Cohen, M. J.; "Qualitative studies of trace constituents by plasma chromatography," *Anal. Chem.* **43 (11)**, 1441-1447 (1971).

Karasek, F. W.; Hill, H. H., Jr.; Kim, S. H.; "Plasma chromatography of heroin and cocaine with mass-identified mobility spectra," *J. Chromatogr*. **117 (2)**, 327-336 (1976).

Karasek, F. W.; Maican, A.; Hill, H. H., Jr., "Air pollution analysis from exposed surfaces by simultaneous ISS/SIMS," Intl. J. of Environ. Anal. Chem., 5(4), 273-92 (1978)

Karpas, Z.; Pllevoy, Y.; Mellous, S.; "Determination of bromine in air by ion mobility spectrometry " *Anal. Chim. Acta* **249 (2)**, 503-507 (1991).

Ko, J. S.; Yoon, H. C.; Yang, H.; Pyo, H. B.; Chung, K. H.; Kim, S. J.; Kim, Y. T.; "A polymer-based microfluidic device for immunosensing biochips," *Lab Chip* **3**, 106–113 (2003).

Lawrence, A. H. and Elias, L., "Application of air sampling and ion-mobility spectrometry to narcotics detection - A feasibility study " *Bull. Narcot.* **37 (1)**, 3-16 (1985).

Lawrence, A. H.; Barbour, R. J.; Sutcliffe, R.; “Identification of wood species by ion mobility spectrometry,” *Anal. Chem.* **63 (13)**, 1217-1221 (1991).

Leasure, C. S. and Eiceman,G. A.; "Continuous detection of hydrazine and methylhydrazine using ion mobility spectrometry", *Anal. Chem*. **57**, 1890-1894 (1985).

Lee, T. W.; Jeon, S.; Maria, J.; Zaumseil, J.; Hsu, J. W. P.; Rogers, J. A.; “Soft-contact optical lithography using transparent elastomeric stamps: Application to nanopatterned organic light-emitting devices,” *Advanced Functional Material* **15**, 1435-1439 (2005).

Lemière, F.; “Interfaces for LC-MS,” Department of Chemistry, University of Antwerp, Belgium, December 2001.

Lim, D. V.; Simpson, J. M.; Kearns, E. A.; Kramer, M. F.; “Current and developing technologies for monitoring agents of bioterrorism and biowarfare,” *Clinical Microbiology Reviews*, 583–607 (2005).

Liu, R. H.; Dill, K.; Fuji, H. S.; McShea A.; **“**Integrated microfluidic biochips for DNA microarray analysis,” *Expert Review of Molecular Diagnostics* **6 (2)**, 253-261 (2006).

Matz, L. M. and Hill, H. H., Jr.; “Evaluation of opiate separation by high-resolution electrospray ionization-ion mobility spectrometry/mass spectrometry”, *Anal. Chem.* **73(8)**, 1664-1669 (2001).

Matz, L. M. and Hill, H. H.; "Separation of benzodiazepines by electrospray ionization ion mobility spectrometry-mass spectrometry", *Anal. Chimica Acta* **457(2)**, 235-245 (2002).

McDonald, J. C. and Whitesides, G. M.; "Poly(dimethylsiloxane) as a material for fabricating microfluidic devices," *Accounts of Chemical Research* **35 (7)**, 491- 499 (2002) (and references there in).

McGann, W. J.; Jenkins, A.; Ribiero, K.; Napoli, J.; "New high-efficiency ion trap mobility detection system for narcotics and explosives" in *SPIE Proc.* 2092, pp. 64-75 (1994).

McGann, W. J.; Bradley, V.; Borsody, A.; Lepine, S.; "New, high-efficiency ion trap mobility detection system for narcotics and explosives" in *SPIE Proc.* **2276**, pp. 424-436 (1994).

Miller, R. A.; Eiceman, G. A.; Nazarov, E. G.; King, A. T.; "A novel micromachined high-field asymmetric waveform-ion mobility spectrometer," *Semsors and Actuators B* **67**, 300-306 (2000).

Mitrovski, S. M.; Elliott, L. C. C.; Nuzzo, R. G.; "Microfluidic devices for energy conversion: Planar integration and performance of a passive, fully Immersed H_2-O_2 fuel cell," *Langmuir* **20***,* 6974-6976 (2004).

www.novachem.com/ProductServices/ docs/Benzene_MSDS_EN.pdf

http://www.newobjective.com/electrospray/index.html

http://www.ornl.gov/sci/csd/Research_areas/etv/barringer.htm

Pal, R.; Yang, M.; Lin, R.; Johnson, B. N.; Srivastava, N.; Razzacki, S. Z.; Chomistek, K. J.; Heldsinger, D. C.; Haque, R. M.; Ugaz, V. M.; Thwar, P. K.; Chen, Z.; Alfano, K.; Yim, M. B.; Krishnan, M.; Fuller, A. O.; Larson, R. G.; Burked, D. T.; Burns, M. A.; "An integrated microfluidic device for influenza and other genetic analyses," *Lab on a Chip* **5**, 1024–1032 (2005).

Parmeter, J. E.; Hannum, D. W.; Linker, K. L.; Rhykerd, C. L., Jr.; "Overview of explosives detection research and development in department 5848 at Sandia National Laboratories," in *16th Annual NDIA Security Technology Symposium & Exhibition*, (2000).

Ramsey, J. M.; Jacobsen, S. C.; Knapp, M. R.; "Microfabricated chemical measurement systems," *Nature Med.* **1**, 1093-1096 (1995).

Reed, M.; "Micromechanical systems for intravascular drug and gene delivery," in *4th Annual Biomems- Advances in Medical and Analytical Applications*, (2002).

Ritchie, R. K.; Thomson, P. C.; DeBono, R. F.; Danylewych-May, L. L.; Kim, L.; "Detection of explosives, narcotics, and taggant vapors by an ion mobility spectrometry particle detector" in *SPIE Proc.* **2092**, pp. 87-95 (1994).

Roehl, J. and Bacon, T. A.; "Ambient air monitoring for toluene diisocyanate (TDI) using ion mobility spectroscopy (IMS)", in *Proc. 40th Pitt. Conf. Anal. Chem. Appl. Spectrosc.*, Paper #962, (1989).

Russel, D. H.; Experimental Mass Spectrometry. Plenum Press: New York, 1994.

Salgado, J. D.; Horiuchi, K.; Dutta, P.; "A conductivity-based interface tracking method for microfluidic application," *J. Micromech. Microeng.* **16**, 920-928 (2006).

Sanders, J. C.; Breadmore, M. C.; Mitchell, P. S.; Landers, J. P.; "A simple PDMS-based electro-fluidic interface for microchip electrophoretic separations," *The Analyst* **127**, 1558–1563 (2002).

Schmalzing, D.; Adourian, A.; Koutny, L.; Ziaugra, L.; Matsudaira, P.; Ehrlich, D.; "DNA sequencing on microfabricated electrophoretic devices," *Anal. Chem*. **70**, 2303-2310 (1998).

www.sciencelab.com/xMSDS-Methyl_**alcohol**-9927227

Scott, N.R.; "Nanotechnology and animal health," *Rev. Sci. Tech. Off. int. Epiz.* **24 (1)**, 425-432 (2005).

http://www.seenex.com/products/explosive.html

Shaikh F. A. and Ugaz V. M.; "Collection, focusing, and metering of DNA in microchannels using addressable electrode arrays for portable low-power bioanalysis," in *Proc. of the National Academy of Sciences in the United States of America (PNAS)* **103**, pp. 4825-4830 (2006).

Smith, R. M.; Understanding Mass Spectra: A Basic Approach, 2nd Ed. John Wiley & Sons, Inc: New Jersey, 2004.

Snyder, A. P.; Shoff, D. B.; Eiceman, G. A.; Blyth, D. A.; Parsons, J. A.; "Detection of bacteria by ion mobility spectrometry,"*Anal. Chem.* **63 (5)**, 526-529 (1991).

Spangler, G. E. and Epstein, J.; "Detection of HF using atmospheric pressure (API) and ion mobility spectrometry (IMS)," in *38th Conf. Am. Soc. Mass. Spectrom.*, (1990).

Steinfeld, J. and Wormhoudt, J.; "Explosives detection: A challenge for physical chemistry," *Annual Review of Physical Chemistry* **49**, 203-232 (1998).

Steiner, W. E.; English, W. A.; Hill, H. H., Jr.; "Separation efficiency of a chemical warfare agent simulant in an atmospheric pressure ion mobility time-of-flight mass spectrometer (IM(tof)MS)," *Analytica Chimica Acta* **532(1)**, 37-45 (2005).

Tam M. and H. H. Hill, Jr.; "Secondary electrospray ionization-ion mobility spectrometry for explosive vapor detection", *Anal. Chem*. **76**, 2741-2747 (2004).

Verpoorte, E.; "Microfluidic chips for clinical and forensic analysis," *Electrophoresis* **23**, 677- 712 (2002).

Wang, Y.; Vaidya, B.; Farquar, H. D.; Stryjewski, W.; Hammer, R. P.; McCarley, R. L.; Soper, S. A.; Cheng, Y. W.; Barany, F.; "Microarrays assembled in microfluidic chips fabricated from poly(methyl methacrylate) for the detection of low-abundant DNA mutations," Anal. Chem. **75 (5)**, 1130 –1140 (2003).

Webster, J. R.; Burns, M. A.; Burke, D. T.; Mastrangelo, C. H.; "Monolithic capillary electrophoresis device with integrated fluorescence detector," *Anal. Chem*. **73**, 1622-1626 (2001).

http://www.websters-online-dictionary.org/hy/hydrazine.html

Wu, C.; Siems, W. F.; Hill, H. H., Jr.; "Secondary electrospray ionization ion mobility spectrometry/mass spectrometry of illicit drugs," *Anal. Chem.* **72(2)**, 396-403 (2000).

Xu, J.; Whitten, W. B.; Ramsey, J. M.; "Space charge effects on resolution in a miniature ion mobility spectrometer," *Anal. Chem.* **72**, 5787-5791 (2000).

Xu, J., Whitten, W. B., Ramsey, J. M., "Pulsed-ionization miniature ion mobility spectrometer," *Anal. Chem.* **75**, 4206-4210 (2003).

Zaytseva, N. V.; Goral, V. N.; Montagna, R. A.; Baeumner, A. J.; "Development of a microfluidic biosensor module for pathogen detection," *Lab Chip* **5,** 805 – 811 (2005).

Zeleny, J.; "The electrical discharge from liquid points, and a hydrostatic method of measuring the electric intensity at their surfaces**"** *The Physical Review* **3**, 69-91 (1914).

APPENDIX

A. VOLTAGE DROP AT DIFFERENT RESISTORS

Drift voltage is 500 V (Using Table 1 and Fig. 4 in Chapter Five)

Multimeter resistance, $R_1 = 10.0\ M\Omega$

Each circuit resistor has the resistance R_2

So the voltage drop across the equivalent resistor, $V_{eq,\ resistor\ \#\ 1} = I_1\ R_{eq,\ resistor\ \#\ 1}$

$$83.04\ V = I_1\ R_{eq,\ resistor\ \#\ 1}$$

Total resistance in the equivalent circuit,

$$R_{eq\ ,\ tot.} = 2.5\ M\Omega \times 4 + R_{eq,\ resistor\ \#\ 1} = 10.0\ M\Omega + R_{eq,\ resistor\ \#\ 1}$$

Applied drift voltage, $V = 500\ V$

$$= I_1\ .\ R_{eq\ ,\ tot.}$$

$$= I_1\ .\ (10.0\ M\Omega + R_{eq,\ resistor\ \#\ 1})\ ;\ [\text{the unit of } I_1 \text{ is in } \mu A]$$

$$= 10.0\ I_1 + I_1\ .\ R_{eq,\ resistor\ \#\ 1}$$

$$= 10.0\ I_1 + 83.04\ V$$

Hence the current in the equivalent circuit, $I_1 = \dfrac{500 - 83.04}{10.0} = \dfrac{416.96}{10.0} = 41.696\,\mu A$

So, $R_{eq,\ resistor\ \#1} = \dfrac{83.04\,V}{41.696\,\mu A} = 1.992\,M\Omega$

Now,

$$\frac{1}{R_{eq,\ resistor\#1}} = \frac{1}{R_1} + \frac{1}{R_{2,\,resistor\#1}}$$

$$\frac{1}{R_{2,\ resistor\#1}} = \frac{1}{1.992} - \frac{1}{10.0}$$

$$R_{2,\ resistor\#1} = 2.49\ M\Omega$$

Similarly

$R_{2,\ resistor\#2} = 2.485\ M\Omega$

$R_{2,\ resistor\#3} = 2.52\ M\Omega$

$R_{2,\ resistor\#4} = 2.48\ M\Omega$

$R_{2,\ resistor\#5} = 2.47\ M\Omega$

Total resistance in the circuit,

$R_{tot.} = 2.49 + 2.485 + 2.52 + 2.48 + 2.47 = 12.445\ M\Omega$

Current in the circuit, $I = V/ R_{tot.} = 500\ V / 12.445\ M\Omega = 40.176\ \mu A$

Hence Potential drop at different resistors,

$V_{resistor\#1} = I \,.\, R_{2,\ resistor\#1} = (40.176\ \mu A)\ (2.49\ M\Omega) = 100.04\ V$

$V_{resistor\#2} = I \,.\, R_{2,\ resistor\#2} = (40.176\ \mu A)\ (2.485\ M\Omega) = 99.837\ V$

$V_{resistor\#3} = I \,.\, R_{2,\ resistor\#3} = (40.176\ \mu A)\ (2.52\ M\Omega) = 101.24\ V$

$V_{resistor\#4} = I \,.\, R_{2,\ resistor\#4} = (40.176\ \mu A)\ (2.48\ M\Omega) = 99.636\ V$

$V_{resistor\#5} = I \,.\, R_{2,\ resistor\#5} = (40.176\ \mu A)\ (2.47\ M\Omega) = 99.234\ V$

Similarly

Potential drop at different resistors when a drift potential of 1000 V was applied,

$V_{resistor\#1} = I \,.\, R_{2,\ resistor\#1} = 200.07\ V$

$V_{\text{resistor \# 2}} = I \,.\, R_{2,\ \text{resistor \# 2}} = 199.67$ V

$V_{\text{resistor \# 3}} = I \,.\, R_{2,\ \text{resistor \# 3}} = 202.49$ V

$V_{\text{resistor \# 4}} = I \,.\, R_{2,\ \text{resistor \# 4}} = 199.27$ V

$V_{\text{resistor \# 5}} = I \,.\, R_{2,\ \text{resistor \# 5}} = 198.46$ V

Potential drop at different resistors when a drift potential of 1500 V was applied,

$V_{\text{resistor \# 1}} = I \,.\, R_{2,\ \text{resistor \# 1}} = 300.12$ V

$V_{\text{resistor \# 2}} = I \,.\, R_{2,\ \text{resistor \# 2}} = 299.52$ V

$V_{\text{resistor \# 3}} = I \,.\, R_{2,\ \text{resistor \# 3}} = 303.74$ V

$V_{\text{resistor \# 4}} = I \,.\, R_{2,\ \text{resistor \# 4}} = 298.92$ V

$V_{\text{resistor \# 5}} = I \,.\, R_{2,\ \text{resistor \# 5}} = 297.71$ V

Potential drop at different resistors when a drift potential of 2000 V was applied,

$V_{\text{resistor \# 1}} = I \,.\, R_{2,\ \text{resistor \# 1}} = 400.16$ V

$V_{\text{resistor \# 2}} = I \,.\, R_{2,\ \text{resistor \# 2}} = 399.36$ V

$V_{\text{resistor \# 3}} = I \,.\, R_{2,\ \text{resistor \# 3}} = 404.9$ V

$V_{\text{resistor \# 4}} = I \,.\, R_{2,\ \text{resistor \# 4}} = 398.6$ V

$V_{\text{resistor \# 5}} = I \,.\, R_{2,\ \text{resistor \# 5}} = 397.0$ V